Received: 20 December 2022 | Revised: 28 August 2023 | Accepted: 28 August 2023

DOI: 10.1002/ar.25331

SPECIAL ISSUE ARTICLE

The Anatomical Record WILEY

Main morphological characteristics and sexual dimorphism of hominin adult femora from the Sima de los Huesos Middle Pleistocene site (Sierra de Atapuerca, Spain)

José-Miguel Carretero[1,2] | **Laura Rodríguez**[1,3] | **Rebeca García-González**[1] | **Juan-Luis Arsuaga**[4,5]

[1]Dpto. de Ciencias Históricas y Geografía, Laboratorio de Evolución Humana, Universidad de Burgos, Burgos, Spain

[2]Unidad Asociada de I+D+i al CSIC, Vidrio y Materiales del Patrimonio Cultural (VIMPAC), Burgos, Spain

[3]Area de Antropología Física, Departamento de Biodiversidad y Gestión Ambiental, Universidad de León, León, Spain

[4]Centro UCM-ISCIII de Investigación sobre Evolución y Comportamiento Humanos, Madrid, Spain

[5]Facultad de Ciencias Geológicas, Departamento de Paleontología, Universidad Complutense de Madrid, Madrid, Spain

Correspondence
José-Miguel Carretero, Dpto. de Ciencias Históricas y Geografía, Laboratorio de Evolución Humana, Universidad de Burgos, Edificio I+D+i. Plaza Misael de Bañuelos s/n, 09001 Burgos, Spain.
Email: jmcarre@ubu.es

Funding information
Ministerio de Ciencia, Innovación y Universidades, Grant/Award Number: PID2021-122355NB-C31; MCIN/AEI/; Junta de Castilla y León; Fundación Atapuerca

Abstract

The excellent fossil record from Sima de los Huesos (SH) includes three well-known complete adult femora and several partial specimens that have not yet been published in detail. This fossil record provides an opportunity to analyze the morphology of European pre-Neandertal adult femur and its variation with different evolution patterns. Currently, there are a minimum of five adult individuals (males or females). In this study, we compiled previously published basic anatomical and biometric characteristics of SH adult femora, emphasizing the most relevant features compared to other recent and fossil hominins. The SH femora exhibited a primitive morphological pattern common to all non-*Homo sapiens* femora, as well as most of the Neandertal traits. Therefore, the complete Upper Pleistocene Neandertal pattern was well-established in Middle Pleistocene ancestors long before the proper Neandertals appeared. Additionally, we highlight that the SH and Neandertal femora share some morphological traits and proportions with modern humans that hold sexual significance in our species, regardless of size. Keeping this in mind, we discussed the sex determination of the complete SH specimens and re-evaluated sex allocation in two of them.

KEYWORDS

archaic hominins, lower limb, Middle Pleistocene

1 | INTRODUCTION AND OBJECTIVES

The Sima de los Huesos (SH) site is situated deep inside the Cueva Mayor–Cueva del Silo cave system, located in Sierra de Atapuerca (Burgos, Spain), approximately 0.5 km from the present entrance. The site contains bone-bearing breccia with a clayey matrix primarily composed of *Ursus deningeri*, along with human fossils (Aranburu et al., 2017; Arsuaga et al., 2014; Arsuaga, Martínez, et al., 1997). This paleoanthropological site stands out because of the unusually large accumulation

of hominin remains, with a minimum of 29 individuals, and its remote location from karst entrances (Aranburu et al., 2017; Arsuaga, Martínez, et al., 1997; Bermúdez de Castro et al., 2021). The fossil collection found here has been dated to a minimum of 430,000 years ago (Arsuaga et al., 2014).

Since 1976, the SH site has yielded >7000 human remains, which we attributed to *Homo* (hereafter abbreviated as H) *heidelbergensis*, an exclusively European species considered as direct ancestor of Neandertals. This stance has been maintained since the 1990s (Arsuaga et al., 1991, 1993, 1995). However, over the past decade, there has been growing recognition of the problematic nature of this designation, given the large number of derived Neandertal features present in the SH collection, along with the retention of primitive features and general absence of Neandertal features in the Mauer mandible (the holotype of *H. heidelbergensis*; Buck & Stringer, 2014; Manzi, 2011; Mounier et al., 2009; Stringer, 2012; Tattersall, 2011). By examining materials from the SH, *H. heidelbergensis* could be considered a European regional chronospecies, in continuity with *H. neanderthalensis*. However, there are reasons for placing the SH material within the Neandertal clade as a sister group, rather than within *H. heidelbergensis* (Arsuaga et al., 2014, 2015). Other authors (Manzi, 2011; Stringer, 2012; Tattersall, 2011) have suggested more complex scenarios for human evolution in Europe than previously believed. These scenarios involve either significant intraspecific diversity with archeologically distinct settlements, or the coexistence of different lineages with their respective archeological traditions during the Middle Pleistocene (Arsuaga et al., 2014, 2015).

Previous partial analyses of femora from the SH can be found in the studies by Arsuaga et al. (1995, 2015), Carretero et al. (2004, 2012, 2015, 2018), García-González (2013), Rodríguez (2013), and Rodríguez et al. (2018). In this study, we compiled previously published morphological and metrical information on the main anatomical features of the SH adult femora, emphasizing their anatomical clues and within-sample variation. As novelties, we updated the inventory and main metrical variables of the adult specimens, briefly discussed the main features with functional, phylogenetic, and paleobiological interest when possible, and illustrated all specimens and their main anatomical details.

Finally, sexual dimorphism (SD) of the human femur is a widely discussed topic in anthropological literature, as the femur plays an important role in the estimation of physical parameters, such as stature, body mass, and body proportions (Albanese, 2003; Carretero et al., 2012; Feldesman, 1992; Formicola, 2003; Holliday & Ruff, 2001; Holliday, 2012; Trinkaus & Ruff, 2012). However, femoral SD is primarily expressed by differences in size, and to a lesser extent, shape. Robusticity is thought to obscure sexual traits, making the sexual determination of fossil specimens controversial (Plavcan, 1994, 2012). Therefore, we analyzed the SD of the SH femora based on three complete specimens, reassessed their previous sexual diagnoses, and discussed the possible implications.

2 | MATERIALS AND METHODS

This study focused on adult femora from the SH. Updated inventory, basic dimensions, and photographs of the adult specimens were included in this study. Every recognizable fragment of the human bone was labeled AT, followed by an inventory number from one onwards (universal numbering: AT-10, ... AT-93, ... AT-4383). When several fragments fit together, they were named femur (abbreviated as F-), followed by a Roman numeral from I onwards (F-I, ... F-X, F-XI, ...).

To ensure comprehensive comparisons between archaic and recent humans, metric information from 1075 *H. sapiens* adult femora of known sex was collected from published literature and directly from osteological collections (National 1). Additionally, measurements and morphological details of other adult fossil specimens were obtained directly from the original specimens or from the literature (Arsuaga et al., 2015; Carretero et al., 2012, 2018; Rodríguez et al., 2018; Table 1).

The measurements were as described by Martin and Saller (1957). Univariate and multivariate statistical analyses were conducted to explore the sexual and morphological differences between fossils and recent femora. Three-dimensional (3D) reconstructions (ply files) of the SH specimens and 44 complete left femora from the San Pablo collection were created using Mimics software (v21.0, Materialize, Belgium) to measure the angular and curvature variables. The chord and subtense of the femoral shaft curvature, as well as the collodiaphyseal, bicondylar, and torsion angles of the SH and recent specimens, were measured using Autocad Software on 3D reconstructions via computed tomography (CT) (YXLON Compact x-Ray industrial multi-slice CT scanner) available at the University of Burgos (Carretero et al., 2018; Rodríguez et al., 2018). All the variables were tested for normality. Since normality could not be assumed for most of them, the Kruskal–Wallis test was chosen for consistency with all comparative analyses, followed by a Mann–Whitney *U* test when necessary. Besides the size, femoral differences between sexes can also be attributed to femoral relative proportions and shape differences (Albanese, 2003; Asala, 2001; Asala et al., 2004; Cabo et al., 2015; Cavaignac et al., 2016; İşcan & Shihai, 1995; Mahfouz et al., 2007; Purkait & Chandra, 2004; Trinkaus, 1983; Weaver, 2003).

TABLE 1 Recent and fossil samples used for comparisons.

Collection	Origin	Sex[a]	*N*	Source
Ferraz Macedo (Portugal)	European	Male	64	Tamagnini and Vieira de Campos (1949)
		Female	62	
Coimbra (Portugal)		Male	134	This study
		Female	126	
Luis Lopes (Portugal)		Male	35	This study
		Female	32	
San Pablo (Spain)		Male	76	This study
		Female	63	
Hammand-Todd (USA)	African American	Male	36	This study
		Female	30	
Forensic Data Bank (USA)	African American	Male	123	Jantz and Moore-Janzen (2000)
		Female	76	
	Hispanic	Male	15	
		Female	4	
	Melanesian	Male	7	
		Female	3	
	Euroamerican	Male	214	
		Female	136	
Neandertal sample	La Ferrassie 1	Male		By the authors Heim (1982)
	La Ferrassie 2	Female		
	La Chapelle aux Saints	Male		By the authors Boule (1911)
	Spy 1	Female		By the authors Heim (1982)
	Spy 2	Male		
	Neandertal 1	Male		By the authors Heim (1982)
	Amud 1	Male		Endo and Kimura (1970), Heim (1982)
	Fond-de-Forêt	Male		Heim (1982)
	Las Palomas 77	Female		Plavcan et al. (2014), Ruff et al. (2018)
	Las Palomas 96	Female		
	Sidrón 1609	Male		Plavcan et al. (2014), Ruff et al. (2018)
	La Quina V	?		By the authors Heim (1982)
	Shanidar sample			Trinkaus (1983)
	Tabun C1	Female		By the authors McCown and Keith (1939), Heim (1982)
	Regourdou 1	?		Plavcan et al. (2014)
	Kebara 2	Male		Plavcan et al., 2014
	Krapina 207	Male		By the authors Plavcan et al. (2014), Ruff et al. (2018), Trinkaus (2016)
	Krapina 208	Male		
	Krapina 209	Female		
	Krapina 213	Male		
	Krapina 214	Female		

[a]All recent human samples are of known sex except San Pablo, in which the sex has been estimated by the authors based in almost complete skeletons.

Therefore, we explored the utility of certain sexually significant variables in our species when applied to the SH fossil specimens. Specifically, the absolute and relative femoral head sizes, relative distal epiphyseal proportions, bicondylar angles, and loading axis positions were emphasized. Additionally, sex differences in femoral shape within the

TABLE 2 Sex attributed to some fossil specimens based on FHD (in mm) and ordered by increasing FHD.

	Specimen	FH size	Literature sex[a]	Metric data and sexual diagnosis source	Sex logistic regression from modern humans[b]
1	SH F-XVI	41.2	F	Authors; Carretero et al., 2012	F ($p = 0.92$)
2	SH Coxal 1	41.2	F	Arsuaga et al., 1999, 2015; Ruff et al., 2018	F ($p = 0.92$)
3	SH F-XI	41.8	F	Authors; Arsuaga et al., 2015	F ($p = 0.83$)
4	Krapina 207	42.2	M	Trinkaus, 2016; Ruff et al., 2018	F ($p = 0.80$)
5	Palomas 96	43.0	F	Plavcan et al., 2014; Ruff et al., 2018	F ($p = 0.66$)
6	Palomas 92	44.2	F	Plavcan et al., 2014; Ruff et al., 2018	M ($p = 0.60$)
7	Krapina 209	44.3	F	Plavcan et al., 2014; Ruff et al., 2018; Trinkaus, 2016	M ($p = 0.56$)
8	Krapina 214	44.2	F	Plavcan et al., 2014; Ruff et al., 2018; Trinkaus, 2016	M ($p = 0.56$)
9	Tabun C1	44.5	F	Plavcan et al., 2014; Ruff et al., 2018	M ($p = 0.76$)
10	SH- Coxal 1004	45.4	F	Arsuaga et al., 1999, 2015; Ruff et al., 2018	M ($p = 0.82$)
11	Palomas77	45.6	F	Plavcan et al., 2014; Ruff et al., 2018	M ($p = 0.76$)
12	Kebara 2	45.9	M	Plavcan et al., 2014	M ($p = 0.89$)
13	Regordou 1	45.9	?	Plavcan et al., 2014	M ($p = 0.88$)
14	Ferrassie 2	45.9	F	Plavcan et al., 2014; Ruff et al., 2018	M ($p = 0.89$)
15	SH F-V	46.0	F	Authors; Arsuaga et al., 2015	M ($p = 0.89$)
16	Krapina 208	46.4	M	Plavcan et al., 2014; Ruff et al., 2018; Trinkaus, 2016	M ($p = 0.91$)
17	SH F-IV	46.5	F	Authors; Arsuaga et al., 2015	M ($p = 0.92$)
18	Shanidar 5	47.5	M	Plavcan et al., 2014; Ruff et al., 2018; Trinkaus, 1983	M ($p = 0.98$)
19	SH F-XIII	48.3	M	Authors; Carretero et al., 2012	M ($p = 0.99$)
20	Spy 1	48.4	?	Ruff et al., 2018	M ($p = 0.99$)
21	Fond de Foret 1	48.5	?	Heim, 1982	M ($p = 0.99$)
22	SH F-XII	49.0	M	Authors; Carretero et al., 2012	M ($p = 0.98$)
23	Shanidar 4	49.2	M	Plavcan et al., 2014; Ruff et al., 2018; Trinkaus, 1983	M ($p = 0.99$)
24	Prince 1	49.2	F	Plavcan et al., 2014; Ruff et al., 2018	M ($p = 0.99$)
25	SH-2350 (coxal)	49.7	M	Arsuaga et al., 1999, 2015; Ruff et al., 2018	M ($p = 1.00$)
26	SH-800 (coxal)	49.7	M	Arsuaga et al., 1999, 2015; Ruff et al., 2018	M ($p = 1.00$)
27	SH-835/2501 (coxal)	50.6	M	Arsuaga et al., 1999, 2015; Ruff et al., 2018	M ($p = 1.00$)
28	Amud 1	51.5	M	Plavcan et al., 2014; Ruff et al., 2018	M ($p = 1.00$)
29	Aragó 44	52.0	M	Ruff et al., 2018	M ($p = 1.00$)
30	Neandertal 1	52.2	M	Plavcan et al., 2014; Ruff et al., 2018	M ($p = 1.00$)
31	La Chapelle	52.4	M	Plavcan et al., 2014; Ruff et al., 2018	M ($p = 1.00$)
32	Sidron 1609	52.5	M	Plavcan et al., 2014; Ruff et al., 2018	M ($p = 1.00$)
33	Krapina 213	52.7	M	Plavcan et al., 2014; Ruff et al., 2018; Trinkaus, 2016	M ($p = 1.00$)
34	SH F-X	52.8	M	Authors; Arsuaga et al., 2015	M ($p = 1.00$)

TABLE 2 (Continued)

	Specimen	FH size	Literature sex[a]	Metric data and sexual diagnosis source	Sex logistic regression from modern humans[b]
35	Spy 2	54.0	M	Plavcan et al., 2014; Ruff et al., 2018	M ($p = 1.00$)
36	Ferrassie 1	54.0	M	Plavcan et al., 2014; Ruff et al., 2018	M ($p = 1.00$)

[a]Sex from literature cited in this table.

[b]Probability of sexual assignment (p) of fossil specimens in Table 4 using the logistic regression formula of femoral head size derived from our modern human sample: $\text{Ln}(P/(1-P)) = 0.903 \times \text{FH} - 39.49$.

SH and recent samples were explored using 3D geometric morphometric analysis (GMA).

First, we discuss the femoral head size variation in our recent and fossil samples due to the high SD and widespread use of absolute femoral head size in anthropological studies (Ruff, 2010, 2018a). For this analysis, we collected 36 femoral head values from archaic humans, including those from the SH, Neandertals, and other Middle Pleistocene specimens (Table 2). Some data were reported by Ruff (2010), who derived femoral head sizes from the coxal bone acetabular dimensions, including those of some SH specimens. For our study, all fossil specimens were grouped together as archaic hominins for comparison with recent humans.

In a basic analysis, we evaluated femoral head diameter (FHD) dimorphism in a recent sample of known sexes by performing a unidimensional logistic regression analysis with the FHD. Logistic regression was selected over discriminant analysis when there was only one independent variable and one predictive binary dependent variable. Moreover, this analysis does not require a normal data distribution or equal variance–covariance matrices in the two groups (females and males) (Albanese, 2003). In this type of analysis, the probability (always between 0 and 1) of the response variable (sex) can be calculated (Albanese, 2003). In this case, if the probability is >0.5, the individual can be considered as a male; if it is <0.5, the individual can be considered as a female. We also calculated sex allocation accuracy using an external sample that was not used to derive the logistic regression, specifically, a skeletal-sexed medieval sample from the San Pablo Monastery housed in our laboratory ($n = 136$). The fossil specimens were then sexed based on a regression derived from modern humans, and the results were discussed.

For the bicondylar angle, we used univariate analysis to compare the variation in modern humans with that in a few fossil specimens where it can be calculated. Additionally, a univariate analysis was used to show the values of fossil specimens and variation in modern human samples. The position of the bone-loading axis in the fossil specimens was determined according to Walmsley (1933) and Aiello and Dean (1990). The loading axis indicates the pattern of weight transfer through the femur, which appears to differ between archaic and recent human femora. The former shows a pattern in which the load axis (the vertical line from the femoral head to the bicondylar plane; see below) intersects the anatomical axis of the bone at the distal end of the femur and falls midway between the two distal condyles. In the recent femora, the load axis intersects the anatomical axis higher up the shaft and passes through the distal lateral condyle or even lateral to it.

To correct for statistical problems with ratios, we log-transformed the relative proximal and distal epiphyseal proportions following the methods of Hills (1978) and Smith (2005). Additionally, we checked for normality for each index using the Shapiro–Wilk test. If the normality was rejected, nonparametric statistical analyses (Kruskal–Wallis and Mann–Whitney U tests) were performed for comparison. Analysis of covariance (ANCOVA) was used to evaluate whether the population means of the articular proportions (dependent variable) were equal across sexes (categorical independent variable), while statistically controlling the effects of other continuous variables (covariates; Keppel, 1991). Because of the small sample size of males and females in the fossil specimens, conducting an ANCOVA to assess sexual differences among them was not possible. Instead, regressions derived from pooled sex fossils and recent samples and a residual analysis of each sample were performed to compare the pattern of variation between both samples.

Regarding sex differences in femoral shape explored using the 3D GMA, only complete specimens of the right side were used in this analysis, including those from the SH, where F-XIII from the left side was mirrored previously. We used 11 biologically homologous landmarks following the study by Baek et al. (2013) (Table 3). Femoral landmark data were collected using the Landmark software. These landmarks were introduced into the MorphoJ software package (Klingenberg, 2011). The GMA is a powerful statistical tool widely used in

TABLE 3 Homologous femur landmarks[a] used by Baek et al. (2013) and in this study.

Landmark	Type	Position
1	I	Ligament of the femoral head
2	I	Insertion for *piriformis muscle*
3	I	Insertion for *psoas muscle*
4	I	Lateral projection greater trochanter (most lateral point for the insertion for *quadratus femoral* intersection with *gluteus minimus*)
5	II	Deepest point in the femoral neck
6	I	Medial epicondyle
7	I	Lateral epicondyle
8	II	Most distally projected point of the medial condyle
9	II	Most distally projected point of the lateral condyle
10	II	Most anteriorly projected point in the lateral patellar lip
11	II	Most anteriorly projected point in the medial patellar lip

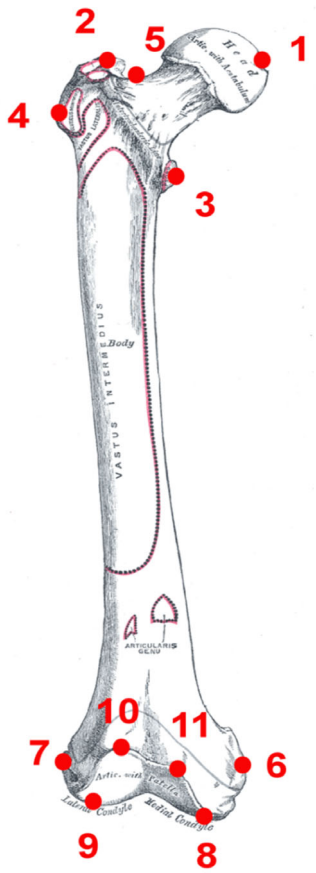

[a]The homologous landmarks type categorization can be found in Bookstein (1991).

morphological analyses, including those in the paleoanthropological field. This eliminates the effect of size, enabling a comparison of shapes between groups based on the spatial relationship between landmarks (Bookstein, 1991; Mitteroecker & Gunz, 2009; O'Higgins, 2000; Slice, 2007). Mahfouz et al. (2007) developed a method based on global shape analysis to determine the shape differences in adult femora according to sex. This method rapidly analyses shape differences across a wide range of femoral sizes. Their algorithm detects dimorphic regions and provides adequate sex discrimination if the landmarks can accurately identify these points.

As mentioned above, 3D reconstructions (ply files) were created using the Mimics software (v18.0, Materialize, Belgium) from CT of 44 complete left femora (24 males and 20 females) from the San Pablo medieval collection. The femora from San Pablo belonged to individuals who were anatomically sexed by the authors because their skeletons were almost completely preserved. Only three complete SH specimens were included in the GMA (F-XIII, mirrored from the right side). The Landmark software IDAV (v3.0, Institute for Analysis and Visualization, 2007) was used to collect the landmarks, which were then introduced into the Morpho-J software package (Klingenberg, 2011). A partial Procrustes superimposition was conducted, which rotated, scaled, and translated the landmark coordinates, enabling an independent study of the size and shape (Bookstein, 1991; Mitteroecker & Gunz, 2009; Zelditch et al., 2004). The landmark error in the analysis was verified and found to be insignificant. To assess the relative variation among modern individuals expressed in Procrustes distance, Procrustes ANOVA was performed using sex as a factor (Klingenberg, 2015; Klingenberg & McIntyre, 1998; Klingenberg et al., 2002). Finally, a Procrustes discriminant analysis (PDA) was conducted to determine the best sexual indicators.

3 | RESULTS

The SH adult femoral sample consisted of 11 different adult specimens, 8 of which were partial and 3 are complete bones (Table 4). These 11 adult specimens represented a minimum of five different individuals based on

TABLE 4 Inventory of the SH adult femora.

N	Specimen	Side	Short description
1	F-IX	R	Distal two thirds of a femur. Distal epiphysis is quite complete
2	F-X	L	Complete femur
3	F-XI	R	Proximal third of a femur
4	F-XII	L	Complete femur
5	F-XIII	R	Complete femur
6	F-XIV	R	Almost complete femur from femoral neck to distal end but lacking femoral head, greater and lesser trochanters, and substantial portions of the distal condyles.
7	F-XXII	R	
7	AT-616	L	Mid-proximal shaft portion with greater trochanter until the beginning of the femoral neck.
8	AT-617	L	Distal epiphysis
9	AT-1020	L	Proximal third of shaft with great trochanter until the beginning of the femoral neck.
10	AT-1802	L	Distal epiphysis and posterior part of distal shaft very damaged. Most of the anterior surface all along the fragment is missing.
11	AT-2470	L	Distal epiphysis

Note: Specimens composition: F-IX = AT-432 + 2461; F-X = AT-612 + 1800 + 4724; F-XI = AT-613 + 1040 + 844; F-XII = AT-665 + 855 + 3042; F-XIII = AT-999 + 2944 + 2943; F-XIV = AT-1529 + 1530 + 1760 + 1770 + 2068.

FIGURE 1 Adult F-IX in anterior (a) and posterior (b) views, and adult F-XI in anterior (c) and posterior (d) views. L, left side; R, right side. Scale in cm.

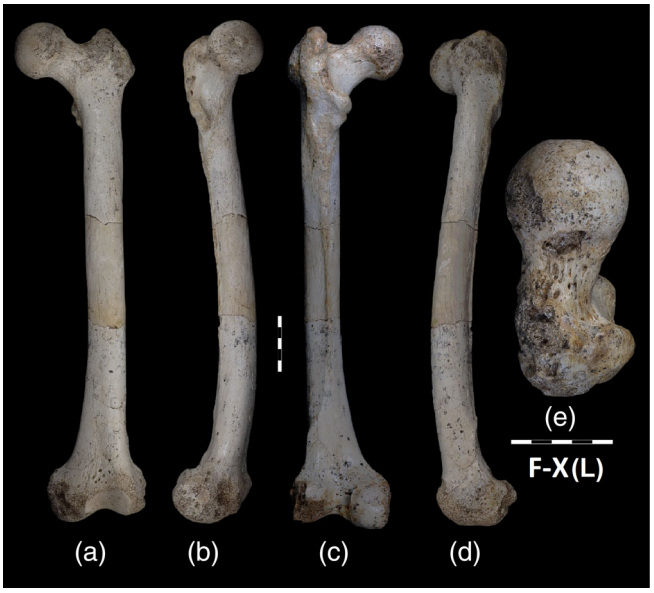

FIGURE 2 Adult F-X in anterior (a), medial (b), posterior (c), lateral (d), and superior (e) views. L, left side. Scales in cm.

the incompatible left distal epiphyses recovered to date: F-X, F-XII, AT-617, AT-2470, and AT-1802 (Figures 1–7).

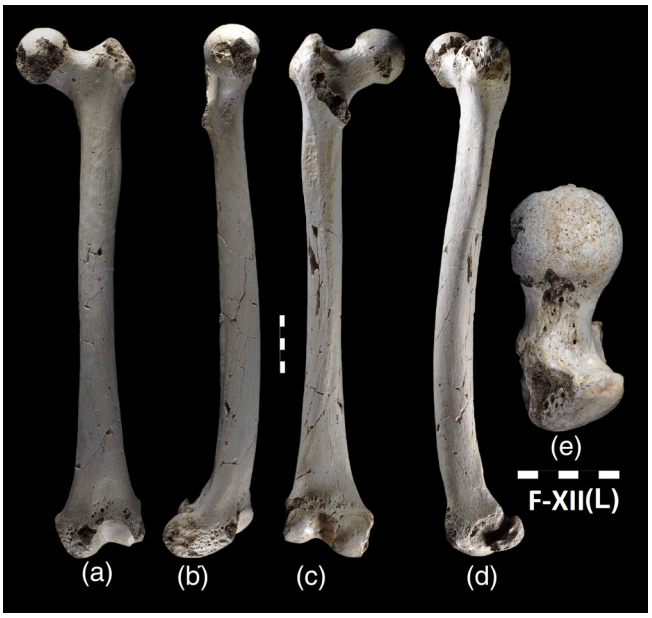

FIGURE 3 Adult F-XII in anterior (a), medial (b), posterior (c), lateral (d), and superior (e) views. L, left side. Scales in cm.

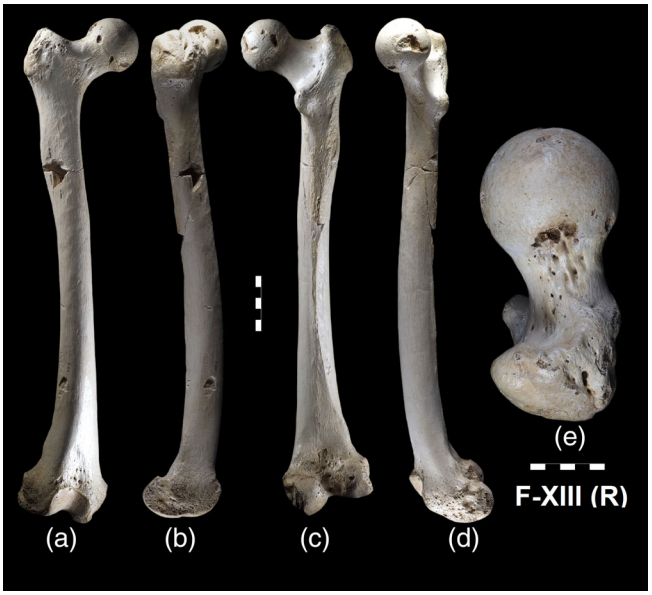

FIGURE 4 Adult F-XIII in anterior (a), lateral (b), posterior (c), medial (d), and superior (e) views. R, right side. Scales in cm.

Table 5 displays the main linear and angular dimensions of the SH adult femora, and Table 6 presents the basic statistics and significance of the comparison test between the SH, Neandertal, and recent human samples. Univariate comparison *p*-values (non-parametric Kruskal–Wallis and Mann–Whitney *U* tests) of the modern and fossil femora indicated significant differences at the proximal, diaphyseal, and distal regions, whereas the Neandertals and SH showed similar dimensional and morphological patterns (Table 6; Arsuaga et al., 2015; Rodríguez, 2013).

FIGURE 5 Adult F-XIV in anterior (a) and posterior (b) views, and adult AT-616 specimens in anterior (c) and posterior (d) views. L, left side; R, right side. Scales in cm.

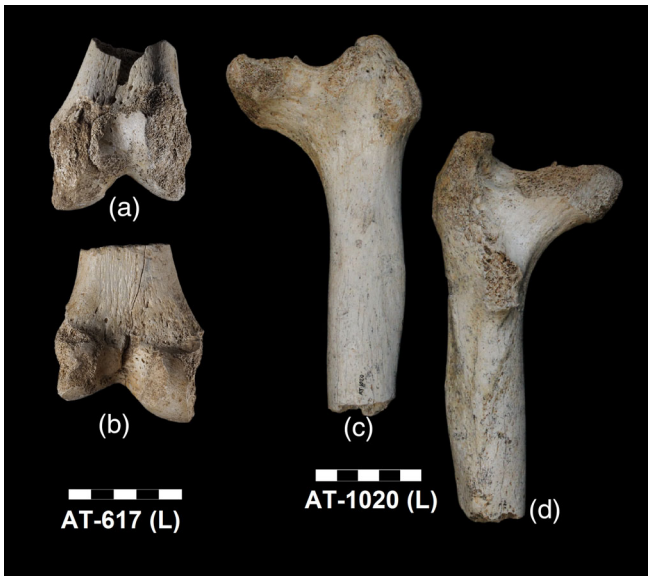

FIGURE 6 Adult distal epiphysis AT-617 in anterior (a) and posterior (b) views, and AT-1020 in anterior (c) and posterior (d) views. L, left side. Scales in cm.

3.1 | Main morphological characteristics of the proximal region

Proximally, all the SH adult femora are characterized by several features: anteroposterior flattening (platymery) of the proximal shaft taken at 80% of the femoral length (below the lesser trochanter about the level of the spiral

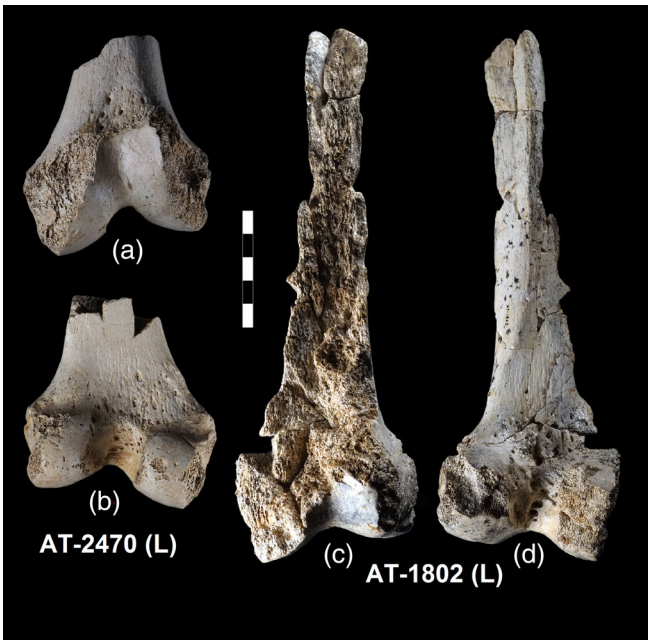

FIGURE 7 Adult distal epiphyses AT-2470 in anterior (a) and posterior (b) views, and the badly fragmented AT-1802 specimen in anterior (c) and posterior (d) views. L, left side. Scale in cm.

line); a well-defined gluteal tuberosity (ridge) along with a large and deep hypotrochanteric fossa, producing a conspicuous lateral projection of the lateral border of the bone, thereby forming the "lateral buttress/crest" (Figures 8 and 9); a robust greater trochanter, well projected proximally and laterally, displaying a strongly developed crest for the gluteus medius on its posterior surface; a well-defined intertrochanteric line on the anterior proximal surface, indicative of a strong iliofemoral ligament and related muscles with insertion in this area (evident in, e.g., the anterior view of F-XI in Figure 1 or AT-1020 in Figure 6) and a robust normally oriented lesser trochanter (F-X shows a bi-lobulated lesser trochanter; Figure 8).

In addition to the hypotrochanteric fossa and gluteal tuberosity, F-X shows, just below the greater trochanter, what appears to be the so-called third trochanter (Aiello & Dean, 1990; Ghosh et al., 2014; Olivier, 1960; Figure 8). No other specimens from the SH exhibited the third trochanter. All the adult SH specimens exhibited well-developed gluteal, pectineal, and spiral lines (Figures 8 and 9). Additionally, most of them (but not all) have a fairly well-developed gluteal tuberosity in the form of a large longitudinal, inflated, blunt, and well-protruded tubercle within the hypotrochanteric fossa, closer to its medial margin (Figure 9). This tubercle is indicative of the extensive development of gluteus maximus. The prominent gluteal ridge that extends along the lateral surface of the greater trochanter in the SH femora is likely a response to strong external hip rotation muscles, including quadratus femoris, gemellus, obturator internus, and even the proximal fibers of the gluteus maximus (Figures 8 and 9).

The femoral neck of the SH femora is anteroposteriorly flattened, and its biomechanical length (Lovejoy, 1975) is relatively large when compared with the maximum length of the bone (Arsuaga et al., 2015; Rodríguez, 2013). This is a well-known primitive trait that also appears in *Australopithecus* and all archaic human femora (Aiello & Dean, 1990; Kennedy, 1983; Ruff et al., 2015). The mean femoral neck length relative to the femoral length (neck-length index; Table 6) of the three complete SH femora (10.5 ± 0.3) is somewhat lower than the mean of the same index in the Neandertal sample (12.0 ± 1.4, $n = 6$), but both are well above the mean of our recent sample (7.9 ± 1.5, $n = 411$; Arsuaga et al., 2015). The collodiaphyseal angle is low compared to recent samples (Arsuaga et al., 2015), a trait shared by Neandertals and other archaic femora (Grine et al., 1995; Trinkaus, 1983; Trinkaus, Churchill, et al., 1999; Trinkaus, Ruff, Churchill, & Vandermeersch, 1998; Trinkaus, Ruff, & Conroy, 1999; Weaver, 2003, 2009). Therefore, the SH specimens showed even lower values ($112.8° \pm 4.0°$, $n = 5$) than the Neandertals ($120.4° \pm 8.9°$, $n = 8$; Table 6). Notably, the variation in this angle within recent human populations may be as great as 23° (Aiello & Dean, 1990; Martin & Saller, 1957), ranging between 115° and 140°, according to Olivier (1960). However, it is equally relevant to mention that the early modern humans of Qafzeh and Skhul display, unlike the SH and Neandertals, had high neck-shaft angles ($131.6° \pm 6.6°$, $n = 4$; Trinkaus, 1993).

Another trait that characterizes most Neandertal femora when compared with recent humans is a larger head (and in general, larger epiphyses) relative to length (Aiello & Dean, 1990; Trinkaus, 1983; Trinkaus, Churchill, et al., 1999; Weaver, 2003, 2009; or De Groote, 2011). This trait is seen in many Neandertals (Arsuaga et al., 2015) and can be observed in the three complete SH femora (Table 6). However, while F-X exhibited an extreme proportion, F-XII and F-XIII were closer to the recent male mean (Figure 10).

3.2 | Main morphological characteristics of the diaphyseal region

In addition to the previously described proximal region, the SH adult femoral diaphysis exhibits the following set of traits: the shaft is robust, as measured by the polar section modulus, Zp (Rodríguez et al., 2018), and displays thick cortical walls; the midshaft index is always around 100%, indicating that the transversal section is rather circular in shape at this level; the linea aspera is well-marked, but there is no true pilaster (Figures 11 and 12); there is a well-pronounced popliteal crest, and the shaft has a high

TABLE 5 Main dimensions of the SH adult femora (in mm and degrees).

Specimen Side	AT-616 L	AT-617 L	AT-1020 L	AT-2470 L	F-IX R	F-X L	F-XI R	F-XII L	F-XIII R	F-XIV R
Maximum length (M1)						458		450	450	
Bicondylar length (M2)						455		442	440	
Vertical head diameter (M18)						52.8	41.8	49.0	48.3	
Neck length (M14c)						47.3	37.4	46.9	48.8	
Neck vertical diameter (M15)			39.2			38.9	27.1	37.2	37.8	
Neck AP diameter (M16)						33.7	22.2	29.3	28.6	
Neck perimeter (M17)						117	86.0	106	105	
Subtrochanteric AP diameter (M10)	32.3		32.0			32.4	25.53	31.0	30.1	30.2
Subtrochanteric ML diameter (M9)	35.9		35.2			37.0	32.79	35.5	34.9	35.7
Midshaft AP diameter (M6)						34.4		32.6	31.9	31.6
Midshaft ML diameter (M7)						34.6		29.7	28.4	29.1
Midshaft perimeter (M8)						105		96.0	93.0	104
Bicondylar breadth (M21)				79.7	89.9	89.4		78.0	79.0	
Lateral condyle AP diameter (M22)		58.5		64.2	65.1	69.8		66.3	67.7	
Medial condyle AP diameter (M24)		49.7		55.3	71.4	60.8		60.0	61.7	
Shaft curvature chord						314.8		310.6	335.6	
Shaft curvature subtense						13.5		13.6	12.6	
Torsion angle (M28)						14°			18°	
Collodiaphyseal angle (M29)						109°	109°	116°	116°	
Bicondylar angle (M30)						9°		13°	13°	
Tangent Condylar angle (M33)[a]				17.5°	11°	10°		11°	11°	

Note: M# refers to the Martin and Saller (1957) variable number. AT-1802 from left side is not in the table because is so badly eroded that none metric dimension can be reasonable directly taken.

[a]In distal view, the angle between the horizontal and the tangent line to the most anterior (superior) points on the medial and lateral condyles (the points that define the trochlear notch). See Figure 14.

degree of anterior–posterior curvature, with the curvature apex set low in the diaphysis (Arsuaga et al., 2015). The SH femora showed a significantly higher degree of femoral curvature subtensity than recent humans ($p < 0.05$) and were similar to Neandertals (p = not significant; Table 6). There were also significant differences in the curvature index between SH, Neandertals, and recent humans, but not between the two fossil samples (Table 6). The high curvature of the SH specimens can be observed in the lateral or medial views of the complete specimens (Figures 2–4).

The SH femora have a relatively thick cortical bone and a relatively small medullary cavity, falling well within the Neandertal range of variation in percentage cortical area (%CA) (Rodríguez et al., 2018). The %CA, which reflects the reinforcement of the diaphysis, was significantly higher in the SH femora than in our recent human sample, especially in the proximal half (65% and 80% levels, $p < 0.01$), although not as much at the mid-distal shaft levels (20%, 35%, and 50%; Rodríguez et al., 2018). The smaller F-XI consistently showed a larger

TABLE 6 Basic statistics and significance of the statistical test for the recent and fossil samples comparisons.

			Normality Shapiro–Wilks			Kruskall–Wallis		Post-hoc Mann–Whitney *U* test		
Linear variables	**Sample**	**Mean ± SD**	***N***	**S-W**	***p*-value**	**K-W**	***p*-value**	**SH-R.H.**	**SH-N**	**N-*R.H.***
Maximum length (M1)	SH	452.7 ± 4.6	3	0.75	*	2.28	Ns	–	–	–
	N	433.3 ± 27.5	13	0.99	Ns					
	R.H.	433.2 ± 32.4	413	0.96	**					
Bicondylar Length (M2)	SH	452.6 ± 4.6	3	0.85	Ns	0.58	Ns	–	–	–
	N	434.1 ± 28.6	10	0.98	Ns					
	R.H.	442.9 ± 34.5	413	1.00	*					
Vertical head diameter (M18)	SH	47.6 ± 5.0	6	0.86	Ns	19.43	**	Ns	Ns	**
	N	49.0 ± 4.0	19	0.93	Ns					
	R.H.	44.5 ± 3.7	414	0.99	**					
Neck length (M14c)	SH	43.6 ± 5.7	5	0.77	*	26.12	**	**	Ns	**
	N	51.9 ± 8.8	7	0.97	Ns					
	R.H.	34.0 ± 6.4	414	0.99	**					
Neck vertical diameter (M15)	SH	34.9 ± 5.3	6	0.80	*	11.17	**	Ns	Ns	**
	N	35.2 ± 2.4	9	0.83	*					
	R.H.	32.1 ± 3.3	416	1.00	Ns					
Neck AP diameter (M16)	SH	27.2 ± 5.0	5	0.89	Ns	5.18	Ns	–	–	–
	N	29.1 ± 3.7	9	0.94	Ns					
	R.H.	26.3 ± 3.2	413	0.99	**					
Neck perimeter (M17)	SH	100.2 ± 13.4	5	0.89	Ns	8.41	*	**	Ns	**
	N	111.2 ± 10.8	6	0.97	Ns					
	R.H.	97.1 ± 10.5	348	0.89	**					
Midshaft AP diameter (M6)	SH	38.1 ± 5.1	6	0.98	Ns	21.47	**	*	Ns	**
	N	31.6 ± 3.1	13	0.97	Ns					
	R.H.	27.5 ± 2.8	416	0.99	*					
Midshaft ML diameter (M7)	SH	29.2 ± 3.1	6	0.90	Ns	29.59	**	*	Ns	**
	N	30.5 ± 2.3	14	0.94	Ns					
	R.H.	26.2 ± 2.8	416	0.98	**					
Midshaft Perimeter (M8)	SH	94.8 ± 11.0	7	0.83	Ns	21.25	**	**	Ns	**
	N	95.4 ± 7.9	13	0.95	Ns					
	R.H.	84.7 ± 7.3	350	1.00	Ns					
Subtrochanteric AP diameter (M10)	SH	29.9 ± 2.6	9	0.83	*	26.24	**	**	Ns	**
	N	27.9 ± 2.4	14	0.94	Ns					
	R.H.	27.1 ± 3.0	416	1.00	Ns					
Subtrochanteric ML diameter (M9)	SH	34.9 ± 1.5	9	0.92	Ns	26.24	**	**	Ns	**
	N	34.7 ± 2.4	14	0.98	Ns					
	R.H.	31.3 ± 3.3	416	0.99	*					
Bicondylar Breadth (M21)	SH	78.2 ± 10.5	6	0.87	Ns	7.99	*	Ns	Ns	**
	N	84.3 ± 7.6	8	0.80	*					
	R.H.	76.6 ± 5.8	405	0.99	*					

(Continues)

TABLE 6 (Continued)

Linear variables	Sample	Mean ± SD	Normality Shapiro–Wilks			Kruskall–Wallis		Post-hoc Mann–Whitney *U* test		
			N	S-W	*p*-value	K-W	*p*-value	SH-R.H.	SH-N	N-*R.H.*
Lateral condyle AP diameter (M22)	SH	66.7 ± 5.0	5	0.88	Ns	17.52	**	**	Ns	*
	N	68.8 ± 3.6	4	0.76	*					
	R.H.	59.3 ± 4.3	334	0.99	Ns					
Medial condyle AP diameter (M24)	SH	59.5 ± 5.8	5	0.84	Ns	6.52	*	Ns	Ns	*
	N	63.7 ± 3.5	4	0.79	Ns					
	R.H.	58.1 ± 4.5	336	1.00	Ns					
Shaft curvature chord	SH	320.3 ± 13.4	3	0.87	Ns	3.87	Ns	–	–	–
	N	317.6 ± 28.3	6	0.93	Ns					
	R.H.	297.5 ± 33.4	135	0.98	Ns					
Shaft curvature subtense	SH	13.2 ± 0.5	3	0.79	Ns	19.76	**	*	Ns	**
	N	15.5 ± 3.4	6	0.91	Ns					
	R.H.	8.4 ± 2.9	135	0.98	Ns					
Angles										
Torsion angle (M28)	SH	16.3 ± 2.0	3	0.92	Ns	0.49	Ns	–	–	–
	N	16.3 ± 4.0	4	0.94	Ns					
	R.H.	12.4 ± 12.7	72	0.79	**					
Collo-diaphyseal angle (M29)	SH	112.8 ± 4.0	5	0.78	*	16.0	**	**	Ns	*
	N	120.4 ± 8.9	8	0.80	*					
	R.H.	125.7 ± 7.0	150	0.99	Ns					
Bicondylar angle (M30)	SH	11.7 ± 2.3	3	0.75	**	4.11	Ns	–	–	–
	N	7.6 ± 3.0	4	0.80	Ns					
	R.H.	8.9 ± 3.0	167	0.99	Ns					
Tangent condylar angle (M33)	SH	9.9 ± 1.9	3	0.75	**	14.78	**	**	Ns	**
	N	9.2 ± 3.0	3	0.79	Ns					
	R.H.	4.0 ± 2.6	104	0.96	**					
Indices										
Head-length index	SH	11.0 ± 0.4	3	0.91	Ns	20.66	**	*	Ns	**
	N	11.4 ± 0.7	10	0.93	Ns					
	R.H.	10.3 ± 0.6	412	0.99	Ns					
Neck-length index	SH	10.5 ± 0.3	3	0.88	Ns	24.09	**	**	Ns	**
	N	12.0 ± 1.4	6	0.93	Ns					
	R.H.	7.9 ± 1.5	411	0.99	**					
Midshaft index	SH	108.9 ± 16.1	6	0.94	Ns	22.97	**	*	Ns	**
	N	104.7 ± 9.3	12	0.94	Ns					
	R.H.	105.3 ± 9.9	416	1.00	Ns					
Curvature index	SH	4.1 ± 0.3	3	0.84	Ns	29.84	**	*	Ns	**
	N	4.9 ± 1.2	6	0.89	Ns					
	R.H.	2.8 ± 1.0	135	0.97	**					
Distal breadth index	SH	18.1 ± 1.2	3	0.83	Ns	6.02	*	Ns	Ns	**
	N	19.1 ± 1.6	6	0.97	Ns					
	R.H.	17.7 ± 1.0	404	0.99	**					

TABLE 6 (Continued)

Linear variables	Sample	Mean ± SD	Normality Shapiro–Wilks *N*	S-W	*p*-value	Kruskall–Wallis K-W	*p*-value	Post-hoc Mann–Whitney *U* test SH-R.H.	SH-N	N-*R.H.*
Lateral condyle relative projection	SH	112.5 ± 3.5	5	0.83	Ns	20.35	**	**	Ns	**
	N	108.1 ± 1.6	4	0.79	Ns					
	R.H.	102.2 ± 4.5	329	0.99	Ns					

Note: Modern humans and Sima de los Huesos samples by the authors. Neandertal sample as in Table 1. Mean of only three males: Neandertal 1 (5.5°); Spy 2 (7°), and Fond-de-Forêt (6°). There is only one female for this variable. La Ferrassie 2 (12° and 11° right and left side).
Abbreviations: *N*, Nenadertals; ns, no significance; R.H, recent humans; SH, Sima de los Huesos.
*$0.01 < x < 0.05$; **$x < 0.01$.

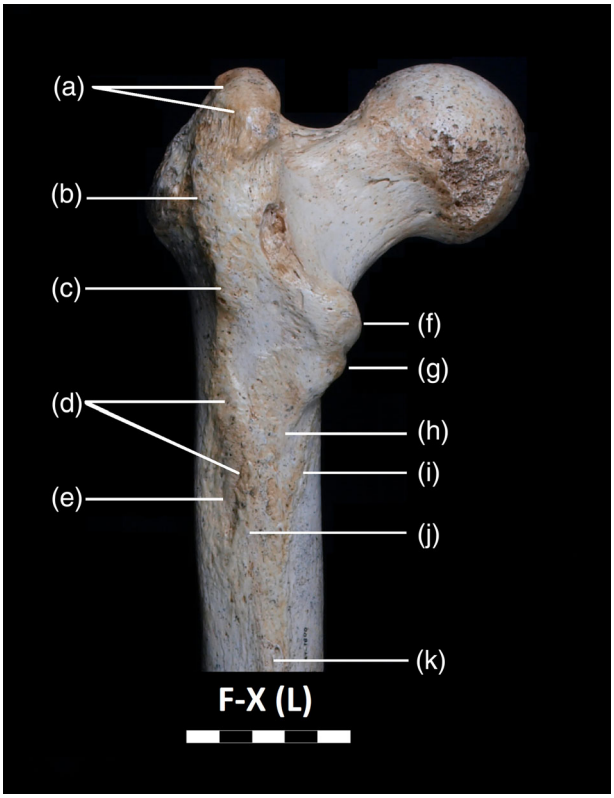

FIGURE 8 Some femoral traits of the proximal region of F-X as an example of SH femoral morphology. (a) Strong transverse crest on the greater trochanter for the m. gluteus medius; (b) strong longitudinal crest along the greater trochanter, probably related with a strong hip external rotation muscles (quadratus femoris, gemellus, and obturator internus) and even the proximal fibers of gluteus maximus; (c) possible third trochanter; (d) strong gluteal tuberosity as a longitudinal tubercle for the insertion of the m. gluteus maximus; (e) hypotrochanteric fossa; (f,g) superior and inferior lobes of the bilobulated lesser trochanter; (h) pectineal line; (i) spiral line; (j) gluteal line; and (k) posterior border of linea aspera. L, left side. Scale in cm.

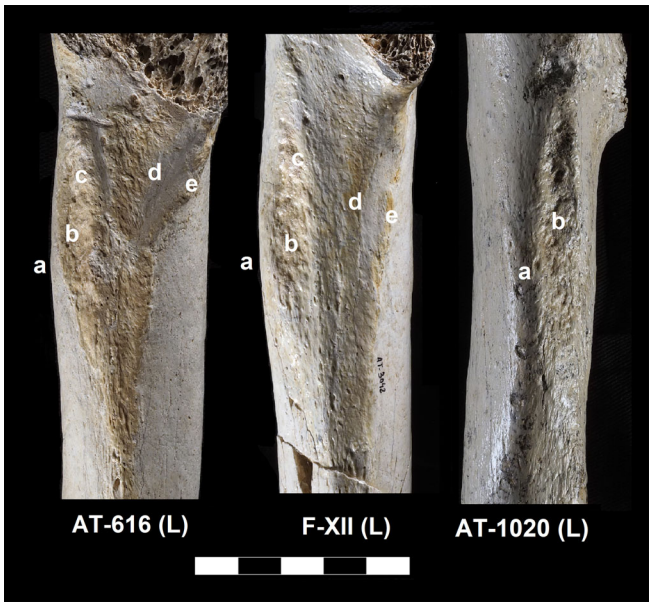

FIGURE 9 Postero-proximal region of three SH femora showing the hypotrochanteric fossa, the gluteal tuberosity close to its medial border and lateral buttress. AT-216 and F-XII are in posterior view. AT-1020 is in lateral view to emphasize the lateral buttress; (a) protruded lateral border or what we call lateral buttress; (b) deep hypotrochanteric fossa; (c) strong gluteal tuberosity tubercle; (d) pectineal line; and (e) spiral line. L, left side. Scale in cm.

%CA (relatively thicker cortices) along the shaft compared to that in the larger SH specimens, a pattern of SD found in *H. sapiens* groups (Rodríguez et al., 2018). It is also noteworthy that F-XIII had a relatively thicker cortex than did F-IX and F-X (Figure 12). The SH femur presents a medial cortical thickening at the midshaft (medial buttress; Rodríguez et al., 2018), associated with the lack of a real pilaster. This feature is also frequent in other archaic femora (Trinkaus & Ruff, 2012). Additionally, Chevalier and de Lumley (2022) identified a frequent strong midshaft posteromedial reinforcement of the cortical thickness in Neandertals and some, but not all, Middle Pleistocene hominins. For example, based on illustrations from Rodríguez et al. (2018), these authors detected that the midshaft femoral

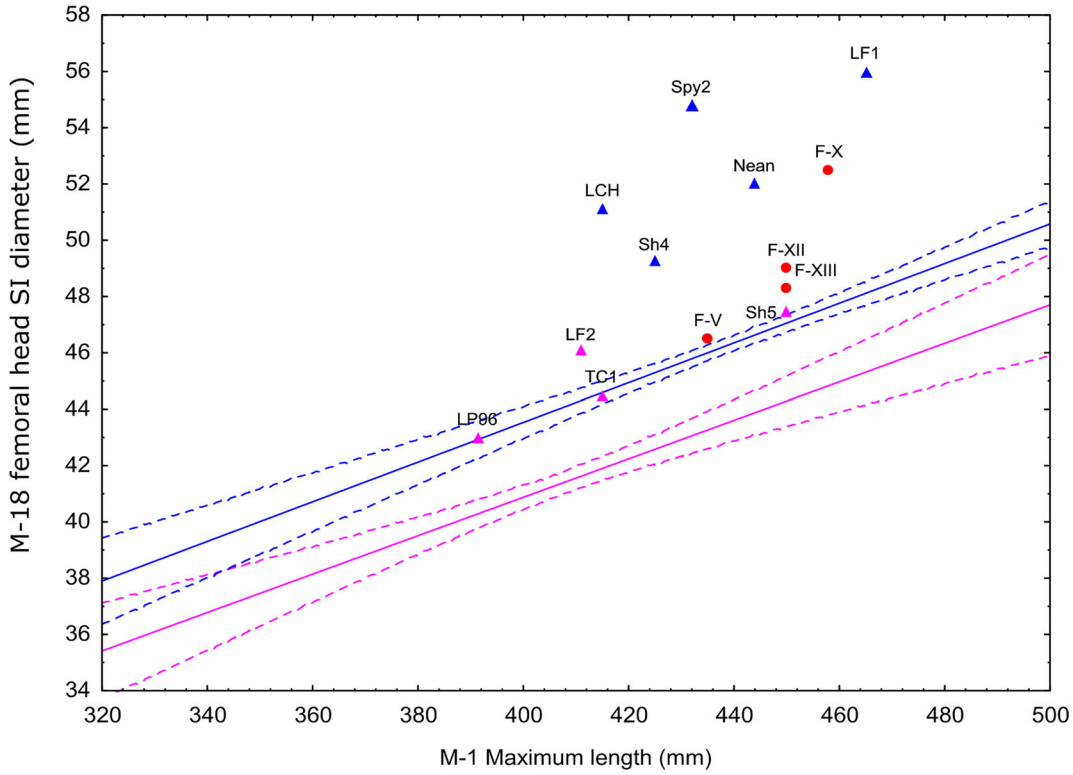

FIGURE 10 Femoral head diameter on femoral maximum length and ANCOVA analysis: mean and prediction intervals at 95% for our sample of recent females (pink) and males (blue) and the position of the fossil specimens. LCH, La Chapelle aux-Saints-1; LF1, La Ferrassie 1; LF2, La Ferrassie 2; LP96, Las Palomas 96; Nean, Neandertal-1; Sh4, Shanidar 4; Sh5, Shanidar 5; TC1, Tabun C1. F-X, F-XII, and F-XIII femora from Sima de los Huesos. Regression formulae of *H. sapiens* males versus females extracted from ANCOVA: Male FHD = 24.21 + Max. Length × 0.05. For females, we must subtract 4.07 from the result ($p < 0.01$, $r^2 = 0.71$).

pattern in Arago A-141 femur indicates similar cortical bone thickness in each direction, a pattern that, according to Chevalier and de Lumley (2022), is closer to that of *Homo erectus* femora from Trinil and Zhoukoudian.

Most (if not all) of these femoral shaft features have been described as part of the archaic pattern of femoral morphology and can be considered primitive features within the genus *Homo*, including *Homo naledi* (Chevalier & de Lumley, 2018, 2022; Day, 1971; De Groote, 2011; Gilbert, 2008; Heim, 1982; Kennedy, 1983; Marchi et al., 2017; McCown & Keith, 1939; Rosenberg et al., 2006; Ruff et al., 1991, 1993, 2015; Shackelford & Trinkaus, 2002; Trinkaus, 1976, 1983; Trinkaus & Ruff, 2012; Weaver, 2009; Weidenreich, 1941).

The cross-sectional characteristics of the SH femoral diaphysis were similar to those of other Early, Middle, and Upper Pleistocene archaic *Homo* representatives, with a thick cortex and a rounded shape along most of the length of the diaphysis (Rodríguez et al., 2018). In the SH specimens, the anteroposterior ovoid portion was located lower in the diaphysis (35%; Figure 12), in contrast to the modern human pattern, where the anteroposterior ovoid portion was located higher in the shaft (50% and 65%; Rodríguez et al., 2018). The SH and Neandertal femora are close to each other in terms of their standardized cross-sectional modulus (Z), which is well above that of modern human samples (Rodríguez et al., 2018). This is an expression of their high cross-sectional torsional strength, demonstrating the femoral diaphyseal hypertrophy that characterizes these two fossil species. The cross-sectional parameters must be standardized by bone length and estimated body mass; among the SH femora (using the femoral head to estimate body mass; see Table 7), the cross-sectional modulus was much higher in F-IX and F-X than that in F-XIII (Rodríguez et al., 2018). Finally, we would like to note that there are some differences in the section modulus values between those calculated with Autocad software, as in the study by Rodríguez et al. (2018), and the same variables were calculated using Moment-Macro software (C. B. Ruff personal communication). Because of the widespread use of Moment-Macro, Table 8 shows the new values of the SH section modulus at the midshaft calculated using this software.

The bicondylar angle was determined for the three complete SH specimens (Table 5). There has been a large variation in recent human populations, and the three SH femora also showed a large variation in this angle. While F-X has an angle (9°) close to the recent mean, it is much higher in F-XII and F-XIII (13°) and close to the upper limit of modern human distribution (Figure 13a; Table 6). The scarce

FIGURE 11 Three examples of linea aspera among the SH femora. Central portion of the diaphysis of F-X in posterior (a) and medial (b) views and of AT-216 (c) and F-XIV (d) in lateral view. Although linea aspera is well developed, there is no trace of a real pilaster, as is the common condition in *H. sapiens*. AT-216 and F-XIV are the specimens whose linea aspera are more elevated from the posterior surface of the bone, although the morphology does not corresponds to a real pilaster in any of them.

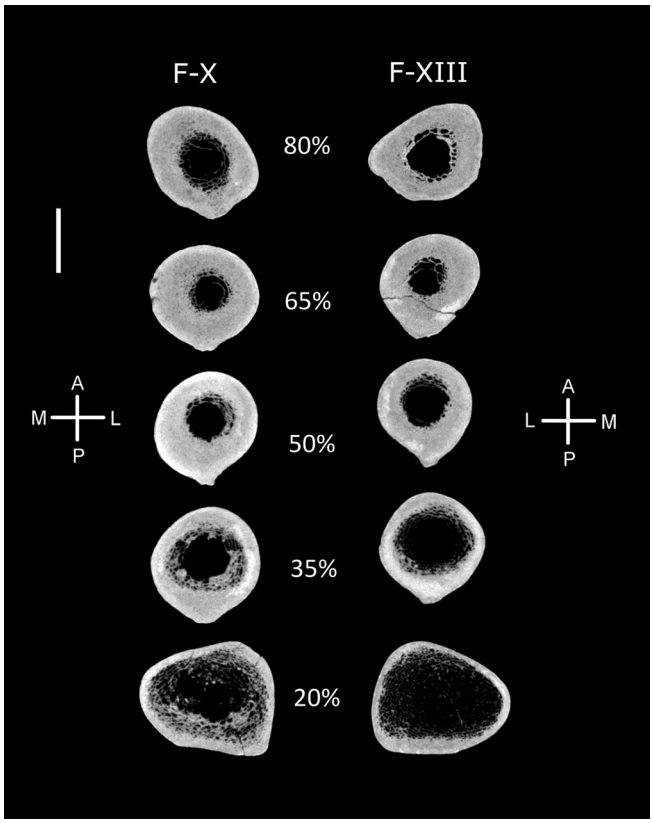

FIGURE 12 Cross sections of F-X and F-XIII at different shaft levels. All the SH femora, either adults or subadults, have cortical thicknesses significantly higher than the *H. sapiens* average. In addition to the thick cortices, the medial wall is thicker than the lateral wall, as is the rule in many archaic femora.

Neandertal evidence places the mean of the three available male specimens ($6.1 \pm 1.5°$; Neandertal $1 = 5.5°$; Spy $2 = 7°$; Fond-de-Forêt $= 6°$; Table 6) well below the values of the single female, La Ferrassie 2 (12° and 11° for the right and left femurs, respectively), and below the recent means (Tables 6 and 9). The femoral load axis is related to the bicondylar angle, as described by Walmsley (1933) and Aiello and Dean (1990). As noted above, in the archaic femora, the load axis intersects the anatomical axis of the bone at the distal end of the femur, whereas in recent femora, it intersects higher up the shaft (Figure 13b). Again, there were clear differences in the load axes among the three complete SH femora. While F-X shows the pattern described for archaic femora, F-XII and F-XIII are modern, human-like (Figure 13b). In terms of the torsion angle, the three SH complete femora showed slightly higher values (Table 5), as in Neandertals, but all were well within the normal modern human variation (Table 6).

3.3 | Main morphological characteristics of distal epiphysis

In the lateral and medial views, the condylar profiles of the SH femora presented a normal posterior extension typical of the human femora. The posterior popliteal triangle (or surface) is normally flattened and not convex, and the medial and lateral epicondyles are blunt with a deep lateral popliteal sulcus and a well-developed medial adductor tubercle (Figure 4b–d).

In the distal view, the most noteworthy trait of the SH femora is the anterior projection of the lateral condyle relative to the medial condyle (Rodríguez, 2013). This describes the degree of proximal projection of the lateral lip and depth of the patellar groove (Figure 14). The patellar groove prevents lateral luxation of the patella. Although not outside the range of recent variations, the SH femora displayed a deep patellar groove with a relatively higher lateral lip because of the significantly more anteriorly projected lateral condyle relative to the medial one. There were significant differences between the fossil and recent samples in the relative proportions of the lateral and medial condyles (lateral condyle relative projection, Table 6). The average difference between the maximum anteroposterior length of the lateral minus medial condyles for the SH sample was 7.2 ± 1.6 mm, with a minimum of 5.9 and maximum of 9.0 mm ($N = 5$). This means that the lateral

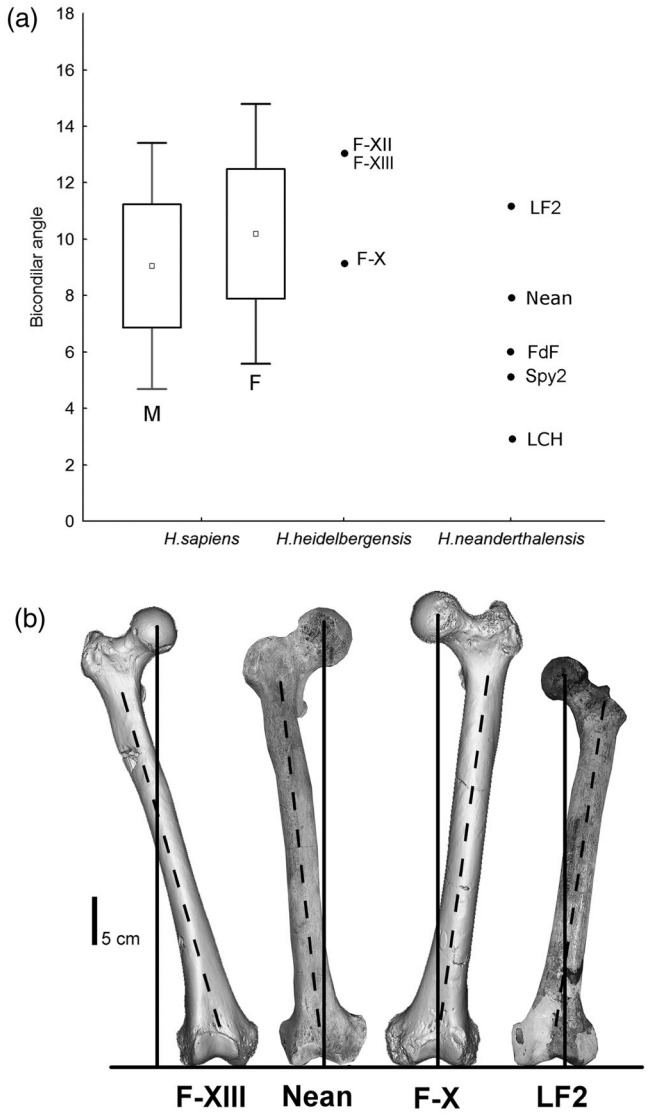

FIGURE 13 (a) Box plot of femoral physiological (bicondylar) angle of our male (M) and female (F) recent samples, SH femora, and some Neandertal specimens. Recent sample means as in Table 4 (males = 9.1° ± 2.2°; females = 10.1° ± 2.3°). Box represent one standard deviation; bar represents the sample range. Fossil data taken by the authors on pictures or 3D images: LF2, La Ferrassie 2 (11°); Nean, Neandertal 1 (7.8°); Spy2 (5°); FdF, Fond-de-Forêt (6°). F-X (9°), F-XII (13°) and F-XIII (13°) femora from Sima de los Huesos. We just note that females display greater angles than males in the three groups. (b) Femoral loading axis position in Sima de los Huesos F-X and F-XIII, and in Neandertal 1 (male) and La Ferrassie 2 (female) Neandertals. Loading axis is the vertical line from the femoral head to the bicondylar plane—and both, the position of the point of the shaft where loading axis intersects with the diaphyseal anatomical axis, and the point where reach the bicondylar plane were determined.

condyle projects 11% more than the medial condyle on average. In contrast, in a large recent human sample, the average difference between the distal condyles is only 1.2 mm (i.e., 2% of the difference between the condyle's projection). Trinkaus (2000) reported that the lateral patellar trochlear margins project 10% more than their medial margins in four sufficiently complete Neandertal distal femora. An early modern human sample had a mean of 3% ($n = 5$) and two recent human samples provided means of 6.2% and 4.9%, respectively, similar to the 2% difference found in a large recent sample. Moreover, an elevated condylar tangent angle was a sign of this trochlear morphology, and was also high in the SH femora (Table 6).

Finally, compared with recent humans, the distal epiphyseal breadth of the adult SH specimens was larger relative to the maximum length (distal breadth index in Table 6; Figure 15; Arsuaga et al., 2015; Carretero et al., 2012; Rodríguez, 2013). Although there was no statistical difference in the slope between the sexes in our recent sample ($p = 0.75$), there was a significant difference in the intercept ($p < 0.01$). Current human males have been shown to have a greater distal epiphyseal width than females for the same maximum length. For the three SH femora, the comparison between the large F-X and smaller F-XII and F-XIII was again key. These two later SH femora have proportions closer to recent males, as does the neandertal female from La Ferrassie 2, whereas F-X is again a clear neandertal-like male in this proportion (Figure 15).

3.4 | Body size estimations

The estimation of adult stature from skeletal remains provides an indication of an individual's size and influences body mass estimation. Carretero et al. (2012) discussed the methodological issues involved in these estimates and reported SH values for the upper and lower limb bones. The mean stature of the entire SH sample was reported to be 163.6 cm. For the complete adult femora, the estimated stature of F-X was 170 cm, whereas that of F-XII and F-XIII was 167 cm. These three femora are considered male (Carretero et al., 2012).

The femur is commonly used to calculate body mass, but different methods can be employed to calculate this parameter (Auerbach & Ruff, 2004; Plavcan et al., 2014; Ruff, 2000; Ruff & Niskanen, 2018), leading to substantial differences in the results (Arsuaga et al., 2015; Carretero et al., 2015, 2018). For example, in Table 7, we can see the results of the body mass estimation for some of the SH specimens, assuming that the three complete femora belong to males. Additionally, the femoral heads of F-IV, F-V, and F-XVI were included in the table, which were completely fused to the shaft, although they belonged to sub-adult bones because the distal end was not fused. The estimates for F-X vary between 81 and 83 kg using FHD, 92 and 94 kg using stature and biiliac breadth, and 99 and 102 kg using bone volume and skeletal weight. In

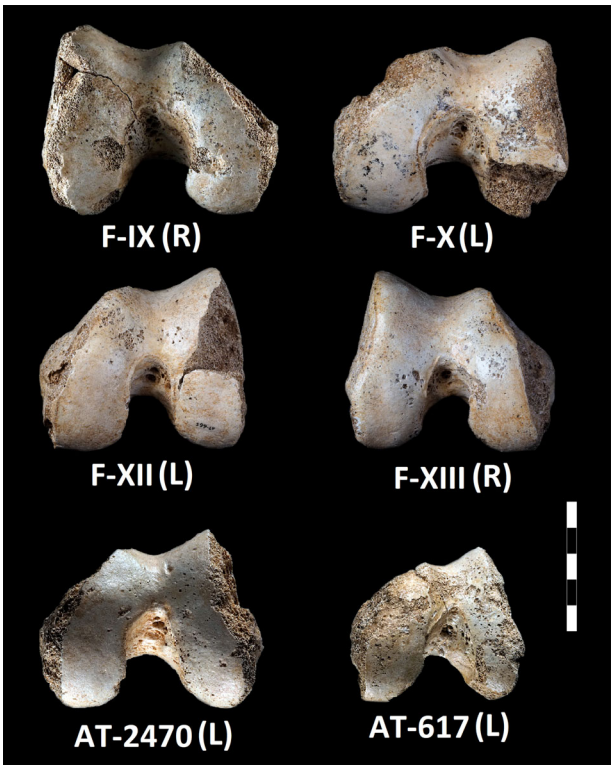

FIGURE 14 Distal view of the lower epiphyses of some SH adult femora. Scale in cm.

TABLE 8 Section modulus at midshaft of SH adult femora computed with Moment Macro.[a]

Specimen	Section level	Zx (mm^3)	Zy (mm^3)	Zp (mm^3)
F-IX	50%	3086	2939.1	5676
F-X	50%	2993	3124	5938
F-XIII	50%	1872	1896	3524
F-XIV	50%	2484	2238	4153

[a]https://www.hopkinsmedicine.org/fae/mmacro.html

the case of F-XIII, the estimates vary between 70 and 74 kg using the FHD and 87 and 88 kg using the skeletal weight (Table 7).

However, it is important to consider SD when interpreting stature and body mass estimates and their palaeobiological implications (Ruff & Niskanen, 2018). All the morphological femoral traits mentioned earlier, which provide mechanical advantages when carrying larger body masses (Ruff et al., 2018), support the large body mass estimates for SH hominines (Carretero et al., 2018; Table 7). If F-XII and F-XIII are considered to represent females rather than males in the SH population, these large body mass estimates could have significant paleobiological implications.

TABLE 7 Body mass (BM) in kilograms of SH hominins relying on different regression formulae.

	Possible sex	Femoral head, diameter (mm)	BM from femoral head diameter, females[a]	BM from femoral head diameter,[a] males	BM from femoral head diameter,[b] pooled sex	BM from stature-biiliac, breadth[c]	BM from stature-biiliac breadth[d]	BM from skeletal weight[e]	BM from femoral weight[e]
F-IV[f]	F	46.5	69.9	–	69.0				
F-V[f]	F	46.0	68.8	–	67.8				
F-X (M)	M	52.8	–	80.8	83.3				
F-X + pelvis 1[g]	M	–	–	–	–	92.5	93.8	99.4	102
F-XI	F	41.8	59.7	–	58.3				
F-XII[h]	M/F	49.0	75.4	71.5	74.6				
F-XIII[h]	M/F	48.3	73.9	69.7	73.0			86.8	88.2
F-XVI	F	41.2	58.4	–	56.9				

Note: Formula for males: BM = (2.741 × FHD − 54.9) × 0.90; $r = 0.50$; Formula for females: BM = (2.426 × FHD − 35.1) × 0.90; $r = 0.41$.

[a]Based on femoral head diameter (FHD) body mass estimation equations in Ruff et al. (1997) and Auerbach and Ruff (2004).

[b]Based on femoral head diameter (FHD) body mass estimation equation in Grine et al., 1995. Formula for pooled sex sample: BM = 2.268 × FHD − 36.5.

[c]Based on Stature/Biiliac breadth regression formula in Ruff et al., 1997. Formula for males: BM (kg) = 0.373 × ST (cm) + 3.033 × LBB (cm) − 82.5; $r = 0.90$.

[d]Based on Stature/Biiliac Breadth regression formula in Ruff et al., 2005. Formula for males: BM (kg) = 0.422 × ST (cm) + 3.126 × LBB (cm) − 92.9; $r = 0.913$.

[e]Based on regression formulae derived from skeletal weight and femur weight of Baker and Newman (1957) in Carretero et al. (2018).

[f]F-IV and F-V have the femoral head completely fused with the proximal diaphysis but not yet the distal epiphysis (Table 2, Figures 11 and 12).

[g]Pelvis 1 skeletal biiliac breadth (SK-BIB) = 34 cm; Living Biiliac Breadth (L-BIB) = 1.17 × SK-BIB − 3.0 (Ruff et al., 1997); Pelvis 1 L-BIB = 36.8 cm; Stature for F-X = 170 cm; stature for F-XIII = 167.8 cm (Carretero et al., 2012).

[h]Weight has only been calculated for the assumed sex of each femur except for F-XII and F-XIII, which have been previously considered as males but could be females as discussed in this paper.

3.5 | SD of the complete SH femora

In this study, all femoral variables used, except the torsion angle, showed significant absolute differences between males and females in a large recent sample (Table 9). Additionally, shape differences (indices) were detected among the recent femora that had sexual significance within our species and could potentially help distinguish between sexes among fossil femora.

For instance, females tended to have a larger bicondylar angle than males, and significant sex differences were found in the recent sample (Table 9). As mentioned earlier, the bicondylar angle was much higher in F-XII and F-XIII (13°) compared than in F-X (9°) (Figure 13a), suggesting that this difference may be attributable to sex variation. Within the entire SH femoral sample, seven femoral heads were measured, although three of them belong to subadult bones (Table 7). Based on their absolute FHD and following recent standards, F-XI and F-XVI were clearly identified as female specimens (FHD of 41.8 and 41.2 mm, respectively). However, the three complete femora (F-X, F-XII, and F-XIII), as well as the subadults F-IV and F-V, were classified as males with a high probability (Table 3).

Moreover, it has been well-established that Neandertals and other representatives of the archaic *Homo* have larger absolute and relative femoral heads than modern humans (M18 and the head length index in Table 6). Logistic regression analysis of the femoral head size derived from the large recent sample in this study classified 85% of the fossil specimens ($N = 36$) as males (Table 3), with an average correct classification rate of 88.5%. Only five specimens (F-XI, F-XVI, and Coxal 1 from SH, Las Palomas 96, and Krapina 2017) were classified as female, all of which had absolute FHD values between 41 and 43 mm. These results suggest potential bias when sexing fossil femora using recent FHD or size standards.

In this study, the relative proximal and distal articular proportions were examined in large recent samples, and clear statistical differences were found between males and females in terms of femoral head size relative to maximum length ($p < 0.01$). Specifically, males tended to have relatively larger femoral heads than females (Figure 10; Cabo et al., 2015). When comparing the SH complete adult femora, a mimetic pattern to the variation between F-X (clearly male based on recent or Neandertal standards), F-XII, and F-XIII was observed. The three SH

TABLE 9 Basic statistics and T-student test between males and females our pooled recent human sample.

Variables (mm and degrees)	Sex	*n*	Mean	SD	SE	*p*-value
Physiological length	M	625	460.4	27.7	1.1	<0.01
	F	464	418.8	27.6	1.3	
Maximum length	M	639	463.8	28.0	1.1	<0.01
	F	474	423.3	27.9	1.3	
Femoral head diameter	M	617	47.3	2.8	0.1	<0.01
	F	458	41.2	2.3	0.1	
Midshaft ML diameter	M	624	27.5	2.6	0.1	<0.01
	F	460	24.1	2.0	0.1	
Midshaft AP diameter	M	559	30.3	2.6	0.1	<0.01
	F	396	26.8	2.3	0.1	
Midshaft circumference	M	422	89.8	7.2	0.3	<0.01
	F	324	80.5	5.6	0.3	
Biepicondylar breadth	M	400	83.8	4.7	0.2	<0.01
	F	260	74.0	4.1	0.3	
Subtrochanteric AP diameter	M	544	28.2	2.6	0.1	<0.01
	F	392	24.8	2.3	0.1	
Subtrochanteric ML diameter	M	555	32.0	3.0	0.1	<0.01
	F	395	28.9	2.3	0.1	
Torsion angle	M	134	12.1	8.0	0.7	0.98
	F	126	12.1	10.4	0.9	
Neck shaft angle	M	134	126.7	5.4	0.5	0.02
	F	126	125.2	5.2	0.5	
Bicondylar angle	M	134	9.1	2.2	0.2	<0.01
	F	126	10.1	2.3	0.2	

specimens have relatively large femoral heads compared to recent human standards, similar to the Neandertals, and therefore they are clearly classified as "recent" males based on this ratio (Figure 10). However, when compared to F-X (and Neandertal males), F-XII, and F-XIII displayed smaller relative head sizes, resembling female-like proportions, and were more similar to those of Neandertal females. Although both SH specimens are longer than the female Neandertal femora, it is important to note that femoral length (stature) is more variable than femoral head size (body weight), at least in recent humans (Ruff, 2000; Ruff et al., 1997). In other words, by recent standards of relative femoral head size, F-XII and XIII from SH are similar to recent males, but by "archaic" standards of this proportion, they could probably be females.

Similar results were obtained when the distal epiphyseal breadth was compared with the maximum length (distal breadth index; Figure 15). Current males tend to have a larger distal femoral epiphysis relative to length compared to females. Female Neandertals, represented by La Ferrassie 2 and Tabun-C1, had relatively smaller distal femoral epiphyses than the available male Neandertals. Comparing F-XII and F-XIII with F-X, the former may be female, displaying relatively smaller distal femoral epiphyses than F-X. In contrast, F-X appeared to be a Neandertal-like male in this proportion (Figure 15).

Regarding the GMA of the femoral shape, the SD was detected in modern humans for both size ($p < 0.01$) and shape ($p < 0.01$). The PDA confirmed these results, showing 100% accuracy in classifying males and females. Differences in landmark configuration between recent males and females indicated that males tended to have lower torsion angles, higher neck-shaft angles, larger proximal and distal epiphyses, wider greater trochanters, and broader intercondylar and patellar notches (Figure 16). The F-X was classified as unambiguously male, whereas F-XII and XIII appeared as unambiguous females when the two SH femora were included in the PDA. These results suggest that the shape differences between F-X and F-XII/XIII from SH are similar to the sexual shape differences observed between modern human males and females (e.g., Baek et al., 2013; Cavaignac et al., 2016; Mahfouz et al., 2007; Figure 17). Although the modern human pattern of sexual differences may not be the best model for application to fossil femora, we believe that sexual variation is a good explanation for the shape differences between F-X and F-XIII/XII.

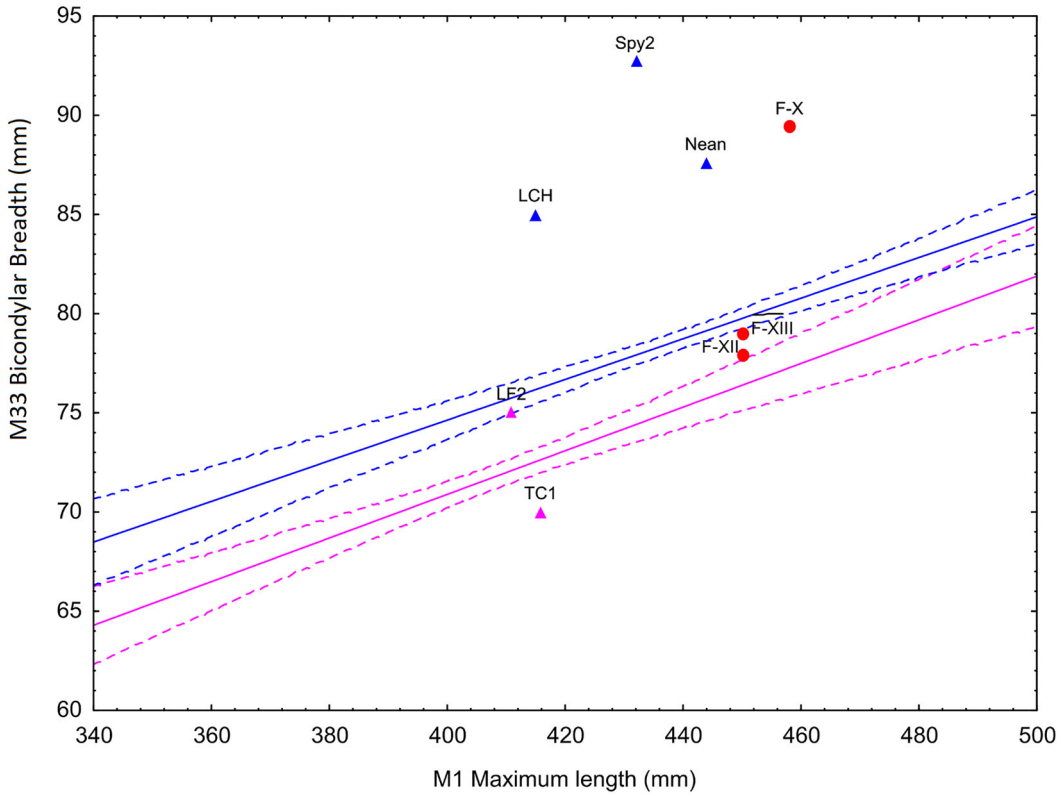

FIGURE 15 Femoral distal epiphyseal (bicondylar) breadth on maximum length and ANCOVA analysis. LF2, La Ferrassie 2; TC1, Tabun C1; Nean, Neandertal-1; Spy2; LCH, La Chapelle aux-Saints-1; F-X, F-XII, and F-XIII femora from Sima de los Huesos. Regression formulae of *H. sapiens* males versus females extracted from ANCOVA: Male Bicondylar Breath = 48.04 + Max. Length × 0.08. For females, we must subtract 7.02 from the result ($p < 0.01$, $r^2 = 0.63$).

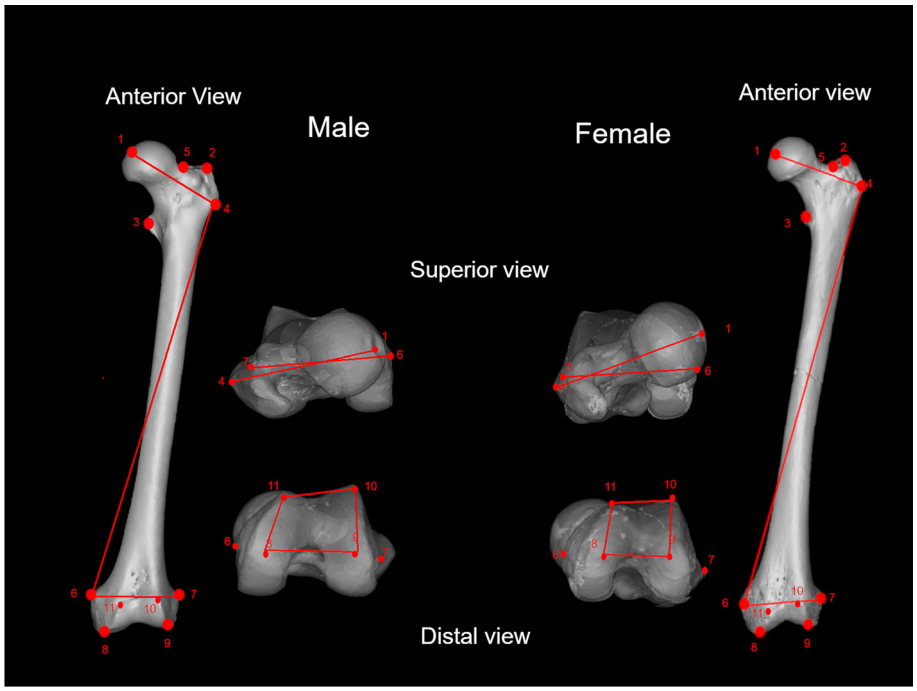

FIGURE 16 Discriminant function landmark configurations of recent femora showing differences in male and female mean shapes.

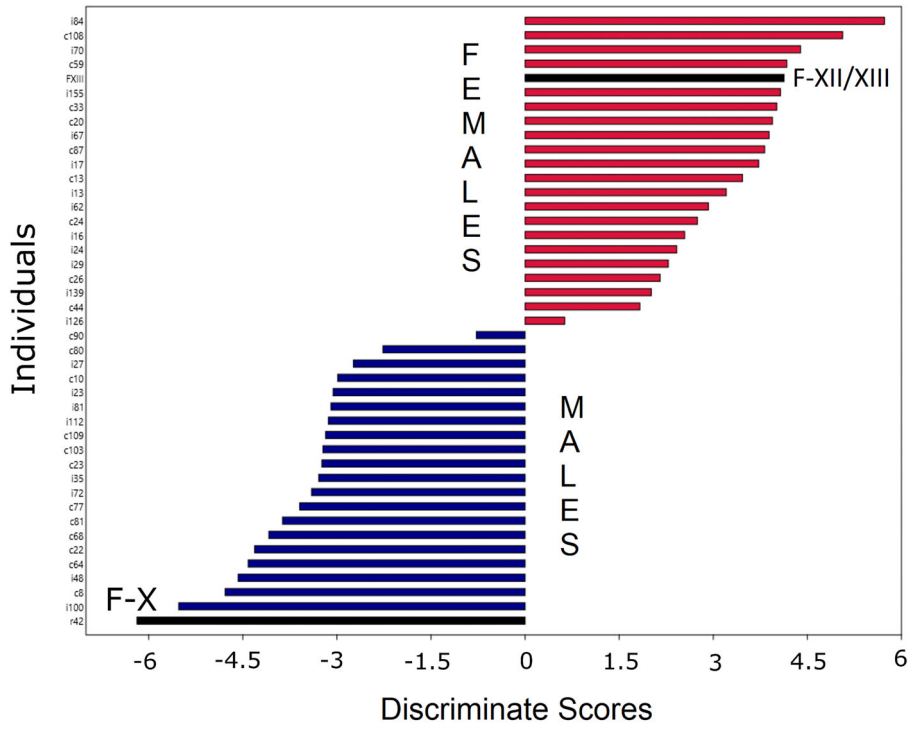

FIGURE 17 Individual scores of the 42 recent specimens from San Pablo (23 males and 19 females) from the discriminant analysis of Procrustes and the position of F-X and F-XIII from SH included as problem cases. Discriminant analysis is based on the Mahalanobis distance ($p < 0.01$).

4 | DISCUSSION

From a phylogenetic perspective, it is well-established that Archaic hominids share a number of characteristics of the femur that make up the primitive morphological pattern of the femur, and that distinguishes them from *H. sapiens* (Aiello & Dean, 1990; Boule, 1911; Day, 1971; De Groote, 2011; Gilbert, 2008; Kennedy, 1983; Lovejoy et al., 2002; Ruff et al., 2015; Trinkaus, 1976, 1983; Weaver, 2003; Weidenreich, 1941). As observed in the SH femora, they display the same morphological traits as other archaic human groups, such as *Homo ergaster*, *H. erectus*, and the Neandertals. This reinforces the notion that the femoral morphology observed in the SH

represents the primitive condition of all archaic large-bodied *Homo* species.

From a paleobiological perspective, these femoral traits have been linked to various factors, including elevated physical activity, different body proportions, and adaptation to cold climates (Pearson & Busby, 2006; Ruff, 1994; Holliday, 1997; Trinkaus, Ruff, & Churchill, 1998; Trinkaus, Ruff, Churchill, & Vandermeersch, 1998; Weaver, 2003, 2009). Although physical mobility patterns can certainly influence these traits (Shaw & Stock, 2010), we believe, in agreement with other researchers (Weaver, 2009), that the morphological pattern observed in archaic femora can be better explained as part of a broader body plan with specific characteristics, such as a broader thorax and hips (Arsuaga et al., 1999, 2015; Bastir et al., 2020; Carretero et al., 2004; García-González et al., 2024; García-Martínez et al., 2014; Gómez Olivencia et al., 2009, 2018), robust and heavier bones (especially the long bones), heavier skeletons, and larger muscular and body masses (Carretero et al., 2018). The homogeneity of morphological traits and their consistent chronological distribution throughout the Pleistocene further supports this interpretation.

4.1 | On morphological traits of proximal region

A hypotrochanteric fossa, associated platymery, and lateral buttress are consistently observed among SH specimens and is highly prevalent in adult and subadult Neandertals (Heim, 1982; Mariotti & Belcastro, 2011; Trinkaus, 1976, 1983). It is also present in the Early Pleistocene femur of *Homo antecessor* from Atapuerca TD6 (Gran Dolina) (Carretero et al., 1999), as well as in other non-European archaic hominins, such as specimens from Olduvai, Daka, Turkana Lake, and Zhoukoudian (Day, 1971; Gilbert, 2008; Kennedy, 1983; Lovejoy et al., 2002; Weidenreich, 1941). Although it is acknowledged that the fossa and platymery are also found in some *H. sapiens* populations (Gilbert, 2008; Hrdlička, 1934, 1937), their significantly higher frequency in archaic hominins during the Early, Middle, and Upper Pleistocene is sufficient to consider them as traits of archaic femora.

This set of proximal traits is associated with high strength load forces in the coronal (mediolateral) plane, which in turn is related to the overall coxo-femoral complex morphology, including a broad pelvis and robust biotype typical of these archaic hominins (Arsuaga et al., 2015; Bonmatí et al., 2010; Carretero, 1994; Carretero et al., 2004).

The flattened and relatively long femoral neck in the SH femora is a well-known primitive trait that is also observed in *Australopithecus* and all archaic human femora (Aiello & Dean, 1990; Kennedy, 1983; Lovejoy, 1975; Lovejoy et al., 1973, 1982; Ruff et al., 2015). Although this represents a limitation for loading of the upper body weight (as longer necks are weaker), it provides enhanced stability to the hip, owing to the action of hip abductors (Kapandji, 1996; Ruff, 1995; Wolpoff, 1978). It is well-established that a relatively longer femoral neck is associated with a larger pelvic biacetabular breadth and pronounced iliac lateral flare (Kapandji, 1996; Lovejoy et al., 1973; Ruff, 1995; Weaver, 2003, 2009), two traits that characterize the pelvis of all archaic *Homo* representatives, including those from the SH (Arsuaga et al., 1999, 2015; Bonmatí et al., 2010; Carretero, 1994). This coxo-femoral configuration in archaic *Homo* reduces the mechanical pressure on the femoral head, but increases the bending diaphyseal stress, which is compensated for by platymery, a lateral buttress, and thicker cortex at the proximal shaft (80% of the femoral length), as seen in the SH femora (Figures 8 and 9).

A longer neck in the femur results in a smaller neck-shaft angle, as documented by Lovejoy (1975) and Lovejoy et al. (1973). In this regard, the adult SH specimens also exhibited low collodiaphyseal angles compared to recent samples (Tables 5 and 6), which is a shared trait between the Neandertals and other archaic femora (Grine et al., 1995; Trinkaus, 1983; Trinkaus, Churchill, et al., 1999; Trinkaus, Ruff, Churchill, & Vandermeersch, 1998; Trinkaus, Ruff, & Conroy, 1999; Weaver, 2003, 2009). Lower collodiaphyseal angles provide lower degrees of joint mobility but are better adapted to support higher body weights (Aiello & Dean, 1990; Kapandji, 1996). These angles have also been correlated with higher activity levels, increased stress in the proximal region of the femoral diaphysis (Aiello & Dean, 1990; Kennedy, 1983; Trinkaus, 1976; Van Gerven, 1972), and enhanced hip stability (Kapandji, 1996; Lovejoy, 1975; Lovejoy et al., 1973; Ruff, 1995, 2005, 2010).

Furthermore, the three complete SH femora displayed relatively large femoral heads, a feature observed in many Neandertals. The key distinction here is that, although F-X exhibits an extreme proportion in this regard, F-XII and F-XIII are closer to the proportions of recent male femora. Our interpretation suggests that this variation may be associated with sex-related differences.

4.2 | On morphological traits of the central diaphysis

Neandertals have been found to exhibit a significantly higher degree of femoral curvature than humans (Arsuaga et al., 2015; De Groote, 2011; Shackelford & Trinkaus, 2002), a characteristic also observed in the SH

femora (Table 6). Curved bones have been suggested to represent an optimal response to both internal (muscle and weight) and external (carrying an object) loadings (Bertram & Biewener, 1988; Lanyon, 1980). In cases where body mass is high, a strongly curved bone can provide mechanical advantages by facilitating muscle packing and compensating for loading bending moments (Currey, 2002). Moreover, femoral curvature appears to be related to repetitive loading on the lower limbs during subsistence strategy-related terrestrial mobility (De Groote, 2011; Holt, 2003; Larsen et al., 1995; Ruff et al., 1991, 1993; Shackelford & Trinkaus, 2002; Stock, 2006; Stock & Pfeiffer, 2004).

As mentioned in Section 3, the SH femora displayed a relatively thick cortical bone and a relatively small medullary cavity (Figure 12). The cortical thickness is influenced by differential endosteal resorption and subperiosteal deposition during development, which reflects the hypertrophy of the Pleistocene human femoral diaphysis (Chevalier & de Lumley, 2022; Pearson & Lieberman, 2004; Shaw & Stock, 2010; Yoshikawa et al., 1994). Moreover, this increased cortical shaft thickness and larger absolute and relative bone volumes are not exclusive traits of the femora, but are observed in the entire lower and upper limb SH adult bones (Carretero et al., 2018) and even in upper limb subadult specimens (García-González et al., 2024). This suggests that there is a strong genetic influence on these characteristics. Shaft entheses, particularly the gluteal tuberosity in the SH femora, which is also common in Neandertals, may imply histological differences from modern humans, likely resulting from genetic differences in development (Mariotti & Belcastro, 2011).

Variations in the cross-sectional properties of long bones have been used to reconstruct the habitual activity behaviors of recent human groups. Studies have shown that factors, such as terrain slope, level and type of physical activity, and mobility may play important roles in shaping cross-sectional properties (Holt & Whittey, 2019; Niinimäki et al., 2017; Pearson, 2000; Ruff, 2000, 2018b; Shaw & Stock, 2010; Sládek et al., 2006; Swan et al., 2020). These findings suggest that the femoral characteristics observed in the SH specimens may provide insights into the physical activities and mobility patterns of these ancient hominins.

Indeed, differences in femoral cross-sectional parameters between Neandertals and recent humans have been a subject of significant interest and debate in the field of paleoanthropology. Previous studies have suggested various factors, such as climate-related habitual behaviors, hip mechanics, mechanical stress, activity levels, and patterning, as potential explanations for these differences (Churchill, 1998; Friedl et al., 2016; Pearson, 2000; Weaver, 2003). However, recent findings by Kubicka et al. (2022) indicated that biological and environmental factors may not fully account for the variation in femoral robustness indicators among Neandertals. This suggests that the Neandertal femur may have responded differently to mechanical stimuli than *H. sapiens*, leading to distinct morphological features in the long bone (Kubicka et al., 2022).

Similarly, a cross-sectional analysis of other geometrical properties of the lower limb in SH hominins, as described by Rodríguez et al. (2018), revealed a pattern and magnitude of robusticity consistent with those of other archaic hominins, including Neandertals. This finding emphasizes body shape and/or high mobility patterns as factors contributing to these femoral traits, which further supports the idea that they represent the characteristic features of archaic large-bodied *Homo* representatives (Gilbert, 2008; Kennedy, 1983; Lovejoy et al., 2002; Trinkaus, Ruff, & Conroy, 1999).

The bicondylar angle is a significant morphological trait in this species, with potential sexual significance (Walmsley, 1933). Interestingly, F-XII and F-XIII from the SH site exhibited even higher values for this angle than La Ferrassie 2, which itself represents the highest angle within the limited available Neandertal sample. This observation led us to hypothesize that the variation between La Ferrassie 2 and the three Neandertal males, as well as between F-XII and F-XIII on one side and F-X on the other, could be attributed to SD. This suggests that sex variation may have played a role in shaping the bicondylar angles of these fossil specimens.

Additionally, the variation in the pattern of the femoral loading axis among the three SH femora, with F-X exhibiting an archaic-like loading pattern and F-XII and F-XIII displaying a more modern human-like loading pattern (Figure 13b), could also be influenced by SD. Finally, the torsion angle, which was very similar among the three complete SH specimens (Table 5), fell well within the normal variation range observed in modern humans and Neandertals (Table 6).

4.3 | Morphological traits of distal region

Distally, the SH femora exhibited a patellar trochlear groove with a relatively higher lateral lip, resulting from the significant anterior projection of the lateral condyle in relation to the medial condyle. This characteristic, also found in Neandertals, suggests a deeper femoral trochlear sulcus and possibly enhanced stability of the patella and entire knee joint. However, the exact implications of these traits are still a subject of debate (Trinkaus, 2000).

In Neandertals, femoral patellar groove asymmetry is accompanied by a patella that possesses more

symmetrical (sub-equal medial and lateral facets) and deeper (more dorsally projected median ridge) articular surfaces than many recent human samples (Trinkaus, 2000; Rosas et al., 2020). These articular patellar traits have been associated with improved patellar stabilization in recent humans (Batra & Aroa, 2014; Cross & Waldrop, 1975; Dejour et al., 1994; Fucentese et al., 2006; Qiu et al., 2022; Zaffagnini et al., 2017). However, Trinkaus (2000) pointed out that the variability in morphology, muscular control, and patellofemoral contact forces observed in extant humans makes it unclear to what extent variations in femoral and patellar articular proportions may affect knee kinesiology.

Finally, in contrast to recent humans, the distal epiphyseal breadth of the SH adult specimens was relatively large in comparison with the maximum length, as indicated by the distal breadth index (Figure 15; Arsuaga et al., 2015; Carretero et al., 2012; Rodríguez, 2013). The notable difference between male F-X, F-XII, and F-XIII, with the latter exhibiting a relatively smaller distal femoral epiphysis than F-X, suggests that this variation could be attributed to sex differences (Figure 15).

4.4 | Sexual dimorphism

Three complete adult femora from the SH (F-X, F-XII, and F-XIII) were previously classified as males because of their large overall size. Their linear dimensions, such as FHD, shaft diameter, shaft perimeter, and distal articular breadth, consistently fell within the range of variation observed in recent males (see Arsuaga et al., 2015; Carretero et al., 2012, 2018; Tables 5 and 9). However, considering the well-known greater skeletal robustness and different body biotype that characterize all large-bodied archaic hominins, including the SH sample (Arsuaga et al., 2015; Carretero et al., 2018), relying solely on size variation for the sexual diagnosis of fossil specimens may not be the most reliable approach (Plavcan, 2012).

Throughout our study, we have identified several femoral shape differences among the SH specimens that have significant sexual implications in our species (Albanese, 2003; Asala, 2001; Asala et al., 2004; Cavaignac et al., 2016; İşcan & Shihai, 1995; Kim et al., 2013; Mahfouz et al., 2007; Plavcan, 2012; Purkait, 2003; Purkait & Chandra, 2004; Ruff, 1987; Steyn & İşcan, 1997; Van Gerven, 1972). These shape differences can be valuable in helping us distinguish between sexes in the SH population, and potentially, in other fossil femora. Specifically, based on the differences discussed earlier (femoral head length and distal epiphyseal length proportions, bicondylar angle, load axis pattern, cross-sectional parameters, and GM femoral shape analysis), it is possible that F-XII and F-XIII represent females in the SH population when compared with F-X. However, it is important to note that these females displayed absolute dimensions and relative epiphyseal proportions that aligned with the male standards. Thus, considering the complexity of SD and body size variation in archaic hominins, the application of multiple morphological indicators is crucial for the more accurate sexing of fossil specimens.

A comparison of femoral head size relative to the maximum length in the Neandertals and modern humans revealed an interesting pattern of sexual variation. On average, Neandertals have larger proximal femoral articulations than modern humans, but this difference is more pronounced in males than in females (Figure 10). However, when specifically examining female Neandertals, such as La Ferrassie 2, Tabun C1, Las Palomas 96, and Shanidar 5, the femoral head index was significantly lower than that of males of their species. This indicates that female Neandertals have relatively smaller femoral heads than male Neandertals. However, compared to our standards, these female Neandertals have femoral head proportions similar to those of recent human males; in fact, based on their absolute and relative femoral head sizes, female Neandertals could easily be classified as recent human males (Figure 10).

We found a similar pattern of sex variation in the relationship between femoral head size and maximum length in the SH femora. Specifically, F-XII and F-XIII showed femoral head proportions that were more similar to those of recent human males than to F-X (Figure 10), suggesting that F-XII and F-XIII could be females compared to F-X, which was classified as a male.

A similar pattern emerged when the distal epiphyseal breadth was compared to the maximum length (distal breadth index; Figure 15). Female Neandertals, such as La Ferrassie 2 and Tabun-C1, have a much smaller distal femoral epiphysis than male Neandertals, similar to the pattern observed in F-XII and F-XIII compared to F-X (Figure 15).

Absolute femoral head size has been recognized as one of the most sexually dimorphic variables of the femur, with females typically having smaller femoral heads than males (Albanese, 2003; Asala, 2001; Dittrick & Suchey, 1986; İşcan and Shihai, 1995; King et al., 1998; Kranioti et al., 2009; Purkait, 2003; Purkait & Chandra, 2004; Srivastava et al., 2012). In our fossil sample, La Ferrassie 1 and Spy 2 have the largest femoral heads at 54 mm, values that are 2.4 and 3.2 standard deviations above the mean of our large recent male sample (47.3 ± 2.8; 38.1–57.0, $n = 617$). The femoral head size of these fossil specimens is among the largest observed in modern humans, with only a few recent males having femoral heads of >55 mm, a limit rarely surpassed in most extant human samples (Plavcan, 2012).

A notable example from fossil records is the large Berg-Aukas male femur from Namibia, with a femoral head size of 56.4 mm (Grine et al., 1995).

Although some differences in the diaphyseal cross-sectional shape of the proximal femora may reflect variations in body shape across Pleistocene human taxa (Ruff, 1991, 1994, 2005; Ruff et al., 1991; Trinkaus, 1993, 2006), it is important to consider the significant differences between males and females in all geometrical diaphyseal cross-sectional parameters. Female individuals, both in recent humans and Neandertals, tend to have a higher % CA than males at most shaft levels (Rodríguez et al., 2018; Ruff, 1987; Trinkaus, 1980; Trinkaus & Ruff, 1999, 2012). This SD is also evident between F-XIII and F-X from the SH specimens (Rodríguez et al., 2018), indicating that the significant differences in cross-sectional geometrical properties between these two SH femora could be due to sexual variation.

Diagnosing the sex of archaic hominins based on pelvic and coxal bone dimensions also presents challenges (Arsuaga & Carretero, 1994; Bonmatí et al., 2010; Bonmatí & Arsuaga, 2007; Rak, 1990, 1991; Rak & Arensburg, 1987; Rosenberg et al., 2006; Tague, 1992; Trinkaus, 1976, 1983, 2016). In such cases, the femoral epiphyseal proportions and FHD distributions can offer additional insights. For example, in some fossil specimens, such as Shanidar 4 and Shanidar 5, the postcranial dimensions are inconclusive with respect to sex, but the morphology of the greater sciatic notch suggests that they should be considered male (Trinkaus, 1983). However, when examining their femoral head size relative to maximum length, Shanidar 4 showed proportions similar to recent males and archaic males, while Shanidar 5 displayed an index more comparable to F-XII and F-XIII from the SH, showing a trend toward female proportions (Figure 10).

Similarly, the Kebara 2 Neandertal has been traditionally attributed to the male sex based on the greater sciatic notch shape, but some authors proposed a probable female status based on its pubic proportions or the condition of the composite arch (Arsuaga & Carretero, 1994; Bonmatí & Arsuaga, 2007; Rak, 1991). Kebara 2 has a femoral head size of 45.9 mm estimated based on the acetabular size (Ruff, 2010). This FHD was identical to that of La Ferrassie 2, lower than that of F-XII and F-XIII from SH (49.0; 48.3), and similar to that of the Palomas 77 (45.6) and AT-1004 (45.5) femora, which are considered females because of their small size (Tables 2 and 6). These findings highlight the complexity of sex determination in fossil records and the importance of considering multiple morphological indicators to assess the sex of fossil specimens accurately.

Determining the sex of fossil specimens based on pelvic and femoral measurements is complex, and in some cases, different indicators may provide conflicting results. For example, the Krapina 207 specimen has greater sciatic notch measurements that place it among males (Bonmatí & Arsuaga, 2007; Trinkaus, 1975, 2016), but the configuration of the composite arches suggests it belongs to a female (Trinkaus, 2016). The estimated femoral head size of Krapina 207 is 42.2 mm, which is clearly within the female range for Neandertals, and even smaller than that of modern humans (Table 9). This is one of the smallest femoral head sizes in the sample used in this study (Table 3). This illustrates that using femoral head size alone for sex determination can be challenging, and that additional morphological indicators must be considered.

The Jinniushan specimen was considered female based on its pelvic and cranial traits, despite having a large absolute coxal bone size (Rosenberg et al., 2006). The size of the Jinniushan ulna also fits better within the range of recent male values than recent female values from many European and Euro-American samples (Carretero et al., 2012). The femoral head size of the Jinniushan female was estimated at 50.2 mm by Rosenberg et al. (2006) (ranging between 49.6 and 50.8 mm) and 49.9 mm by Ruff et al. (2018), indicating that an archaic female could be very close to 50 mm, which is considered extremely rare in extant females. Another example is Grotte du Prince 1, a Middle Pleistocene coxal bone considered to be female (de Lumley, 1972; Rosenberg et al., 2006). However, the estimated femoral head size was equal to that of Shanidar 4 (49.2 cm), which is considered a male. Comparing the data in Table 3 at approximately 49–50 mm, it would be very difficult to make a sex determination based on FHD alone, and as mentioned above, some femur proportions might help distinguish some cases.

Several studies have highlighted that the degree of SD (difference in size between males and females) in recent humans, Neandertals (Trinkaus, 1980, 1983; Weaver, 2009), and the SH hominins (Arsuaga et al., 2015; Arsuaga, Carretero, et al., 1997; Lorenzo et al., 1998) is comparable across these three species. This means that the overall pattern of size variation between males and females is similar, even though the absolute size of individuals might differ because of the larger body size of archaic hominins compared to that of recent humans. The sex diagnosis of F-XII and F-XIII as females in the current study did not contradict this conclusion. This simply reflects the fact that there is a clear offset in size between archaic (male or female) and recent humans, a characteristic feature of the archaic human species. The degree of SD or the average difference in size between males and females could still be similar across these populations, despite differences in absolute size.

Curiously, a review of recent studies that include sexual diagnoses for Neandertal postcranial remains

(Lesnik & Sams, 2014) shows that there is usually a greater representation of males than females. Perhaps the Pleistocene hunter-gatherer groups were composed of quite different numbers of adult males and females, but a recent study on the SD of the enamel and dentin dimensions of permanent canines from the SH (García-Campos et al., 2020) found a sex ratio of 5:9 (males: females) within the dental sample, that is, almost twice as many females as males. However, it is essential to interpret these results with caution and to consider potential biases. The representation of males and females in fossil hominin samples can be influenced by various factors, including taphonomic bias, differences in preservation, and excavation strategies. It is not uncommon to observe a greater representation of males than females in some studies of Neandertal postcranial remains, but this does not necessarily mean that the actual sex ratio within Neandertal populations is skewed toward males. Pleistocene hunter-gatherer groups may have had different patterns of mortality, mobility, and social dynamics, which could have led to the differential preservation and recovery rates of male and female remains.

Rosenberg et al. (2006) noted that Jinniushan is the largest female reported so far in the pre-Holocene record, and the best estimate of her body mass from stature and biiliac width was 79.6 kg; the next largest female in their sample was Grotte du Prince 1, with an estimated body mass of 74.0 kg. For F-XII and F-XIII, we used equations that were independent of sex or body proportions for stature estimates; therefore, we believe that an estimate of 167.8 cm is still valid (Carretero et al., 2012). Body weight, estimated based on the femoral head using the formulas proposed by Grine et al. (1995) for both sexes combined, was 74.6 and 73.0 kg for F-XII and F-XIII, respectively (Table 7; Arsuaga et al., 2015). However, as mentioned above, for F-XIII, the body weight was also estimated at 88.2 kg based on the femur weight and at 86.8 kg based on the estimated skeletal weight (Carretero et al., 2018). These estimates may seem exaggerated for females, but we must consider the greater robustness of archaic hominins, their different and broader body plans, and the likely greater size range of their females, which are more similar to modern males than females. In summary, F-XII and F-XIII from the SH, if females as intended here, could illustrate that large females were probably common and not exceptional in archaic human species.

5 | CONCLUSIONS

The adult SH femora (Figures 1–7) exhibit similar set of morphological features that characterize their evolutionary descendants, the Neandertals. Most (if not all) of these features have been described as part of the archaic pattern of femoral morphology, and can be considered primitive features within the genus *Homo* (including *Homo naledi*).

Proximally, this set of traits includes an anteroposterior flattened neck that is also relatively long with a low-neck angle, and an anteroposterior flattening of the proximal shaft (platymeric) with a constant well-defined and deep hypotrochanteric fossa that produces a conspicuous lateral crest. The shaft is robust, rounded, or transversely elongated in the middle, with thick cortices and no true pilasters. It is also strongly curved anteroposteriorly, with the maximum subtension of the curvature located low in the diaphysis. Distally, there was a strong anteriorly projecting lateral condyle and deep patellar groove. Finally, the relative sizes of the proximal and distal articular dimensions were greater than those of recent femora.

This primitive femoral morphology has been associated with increased physical activity, different body proportions, and adaptation to cold climates; however, we still believe that this primitive femoral pattern is primarily (though probably not exclusively) related to the general body plan of these archaic hominins, which includes a heavier skeleton, broad pelvis, and large body mass. Additionally, we showed that some differences in shape between the three complete adult SH femora suggest a female diagnosis for F-XII and F-XIII, which were previously considered males based on absolute linear dimensions. If F-XII and F-XIII represent females, then large females are likely common in archaic human species. Given the size offset and demonstrated high robustness and absolute larger body size of all archaic hominins, it is more likely that a significant number of archaic females would typically be classified as males using recent human standards of size variation. In contrast, the detection of subtle shape variations in long bones can help improve our ability to diagnose isolated fossil specimens. Femoral shape variation within the SH sample helps to illuminate the problem that size and shape differences confound attempts to assign sex to these archaic hominins, even when other important sources of variation, such as geography, chronology, and phylogeny, are excluded.

AUTHOR CONTRIBUTIONS

José-Miguel Carretero: Conceptualization; investigation; writing – review and editing; methodology; formal analysis; validation. **Laura Rodríguez:** Conceptualization; investigation; methodology; writing – review and editing; formal analysis. **Rebeca García-González:** Conceptualization; investigation; methodology; formal analysis; validation. **Juan-Luis Arsuaga:** Funding acquisition; validation.

ACKNOWLEDGMENTS

We benefitted from fruitful discussions with our colleagues from the Centro UCM-ISCIII sobre Evolución y Comportamiento Humanos of Madrid and Laboratorio de Evolución

Humana at the University of Burgos. We appreciate the Anatomical Record Editorial board for their interest in the Sima de los Huesos (SH) material. We are especially grateful for the help with the English edition of the manuscript and during the publishing process. We thank the anonymous reviewers of the manuscript for their valuable comments. We thank our companions in the Atapuerca research and SH excavation teams for their invaluable dedication to the ongoing work at the SH site. We acknowledge Javier Trueba for the extraordinary graphic documentation of the SH fossils and fieldwork under demanding conditions. We want to thank Maria Cruz Ortega for her extraordinary and patient restoration of the fossils. We thank the following individuals and their institutions for access to the modern and fossil comparative materials: P. Mennecier and A. Froment (Muséum National d'Histoire Naturelle); B. Maureille and C. Couture (Université de Bordeaux 1); Y. Haile-Selassie, B. Latimer, and L. Jellema (Cleveland Museum of Natural History); C. B. Stringer and R. Kruszynski (Natural History Museum, London); J. Radovčic (Croatian Natural History Museum); E. Cunha and A. L. Santos (Coimbra University) and A. Marcal (Bocage Museum). The fossils analyzed in this study are from the "Colección Museística de Castilla y León" of the Junta de Castilla y León.

FUNDING INFORMATION

The Atapuerca research project is financed by the Ministerio de Ciencia, Innovación y Universidades Grant PID2021-122355NB-C31 funded by MCIN/AEI/10.13039/501100011033 and "ERDF A way of making Europe." Fieldwork at the Atapuerca sites is funded by the Junta de Castilla y León and Fundación Atapuerca.

CONFLICT OF INTEREST STATEMENT

The authors declare no conflicts of interest.

ORCID

José-Miguel Carretero https://orcid.org/0000-0003-0409-8087
Laura Rodríguez https://orcid.org/0000-0002-5090-1582
Rebeca García-González https://orcid.org/0000-0002-1035-6655

REFERENCES

Aiello, L. C., & Dean, C. (1990). *An introduction to human evolutionary anatomy*. Academic Press Limited.

Albanese, J. (2003). A metric method for sex determination using the hipbone and the femur. *Journal of Forensic Science*, *48*, 263–273.

Aranburu, A., Arsuaga, J. L., & Sala, N. (2017). The stratigraphy of the Sima de los Huesos (Atapuerca Spain) and implications for the origin of the fossil hominin accumulation. *Quaternary International*, *433*, 5–21.

Arsuaga, J. L., & Carretero, J. M. (1994). Multivariate analysis of the sexual dimorphism of the hip bone in a modern human population and in early hominids. *American Journal of Physical Anthropology*, *93*, 241–257.

Arsuaga, J. L., Carretero, J. M., Lorenzo, C., Gomez-Olivencia, A., Pablos, A., Rodriguez, L., Garcia-Gonzalez, R., Bonmatí, A., Quam, R., Pantoja-Perez, A., Martinez, I., Aranburu, A., Gracia-Tellez, A., Poza-Rey, E., Sala, N., García, N., Alcazar de Velasco, A., Cuenca-Bescós, G., Bermudez de Castro, J. M., & Carbonell, E. (2015). Postcranial morphology of the Middle Pleistocene humans from Sima de los Huesos Spain. *Proceedings of the National Academy of Sciences of the United States of America*, *112*, 11524–11529.

Arsuaga, J. L., Carretero, J. M., Lorenzo, C., Gracia, A., Martinez, I., Bermudez de Castro, J. M., & Carbonell, E. (1997). Size variation in Middle Pleistocene humans. *Science*, *277*, 1086–1088.

Arsuaga, J. L., Carretero, J. M., Martínez, I., & Gracia, A. (1991). Cranial remains and long bones from Atapuerca/Ibeas (Spain). *Journal of Human Evolution*, *20*(3), 191–230.

Arsuaga, J. L., Lorenzo, C., Carretero, J. M., Gracia, A., Martínez, I., García, N., Bermúdez de Castro, J. M., & Carbonell, E. (1999). A complete human pelvis from the Middle Pleistocene of Spain. *Nature*, *399*, 255–258.

Arsuaga, J. L., Martínez, I., Arnold, L. J., Aranburu, A., Gracia-Tellez, A., Sharp, W. D., Quam, R., Falgueres, C., Pantoja-Perez, A., Bischoff, J., Poza-Rey, E., Parés, J. M., Carretero, J. M., Demuro, M., Lorenzo, C., Sala, N., Martinón-Torres, M., García, N., Alcazar de Velasco, A., ... Carbonell, E. (2014). Neandertal roots: Cranial and chronological evidence from Sima de los Huesos. *Science*, *344*, 1358–1363.

Arsuaga, J. L., Martínez, I., Gracia, A., & Carretero, J. M. (1995). Cranial and postcranial remains at the Sima de los Huesos (Sierra de Atapuerca) and human evolution during the Middle Pleistocene. In J. M. Bermúdez de Castro, J. L. Arsuaga, & E. Carbonell (Eds.), *Human evolution in Europe and the Atapuerca evidence* (pp. 283–304). Junta de Castilla y Leon.

Arsuaga, J. L., Martínez, I., Gracia, A., Carretero, J. M., & Carbonell, E. (1993). Three new human skulls from the Sima the los Huesos Middle Pleistocene site in the Sierra de Atapuerca Spain. *Nature*, *362*, 534–537.

Arsuaga, J. L., Martínez, I., Gracia, A., Carretero, J. M., Lorenzo, C., Garcia, N., & Ortega, A. I. (1997). Sima de los Huesos (Sierra de Atapuerca, Spain). The site. *Journal of Human Evolution*, *33*, 109–127.

Asala, S. A. (2001). Sex determination from the head of the femur of South African whites and blacks. *Forensic Science International*, *117*, 15–22.

Asala, S. A., Bidmos, M. A., & Dayal, M. R. (2004). Discriminant function sexing of fragmentary femur of South African blacks. *Forensic Science International*, *14*(5), 25–29.

Auerbach, B. M., & Ruff, C. B. (2004). Human body mass estimation: A comparison of morphometric and mechanical methods. *American Journal of Physical Anthropology*, *125*, 331–342.

Baek, S. Y., Wang, J. H., Song, I., Lee, K., Lee, J., & Koo, S. (2013). Automated bone landmarks prediction on the femur using anatomical deformation technique. *Computer-Aided Design*, *45*, 505–510.

Baker, P. T., & Newman, R. S. (1957). The use of bone weight for human determination. *American Journal of Physical Anthropology*, *15*, 601–618.

Bastir, M., García-Martínez, D., Torres-Tamayo, N., Palancar, C. A., Beyer, B., Barash, A., Villa, C., Sanchis-Gimeno, J. A., Riesco-López, A., Nalla, S., Torres-Sánchez, I., García-Río, F., Been, E., Gómez-Olivencia, A., Haeusler, M., Williams, S. A., & Spoor, F. (2020). Rib cage anatomy in *Homo erectus* suggests a recent evolutionary origin of modern human body shape. *Natural Ecology and Evolution*, *4*(9), 1178–1187.

Batra, S., & Arora, S. (2014). Habitual dislocation of patella: A review. *Journal of Clinical Orthopaedics and Trauma*, *5*(4), 245–251.

Bermúdez de Castro, J. M., Martínez, I., Gracia-Téllez, A., Martinón-Torres, M., & Arsuaga, J. L. (2021). The Sima de los Huesos Middle Pleistocene hominin site (Burgos Spain) estimation of the number of individuals. *The Anatomical Record*, *304*(7), 1463–1477.

Bertram, J. E., & Biewener, A. A. (1988). Bone curvature: Sacrificing strength for load predictability? *Journal of Theoretical Biology*, *131*(1), 75–92.

Bonmatí, A., & Arsuaga, J. L. (2007). The innominate bone sample from Krapina. *Periodicum Biologorum*, *109*, 335–361.

Bonmatí, A., Gómez-Olivencia, A., Arsuaga, J. L., Carretero, J. M., Gracia, A., Martínez, I., Lorenzo, C., Bermúdez de Castro, J. M., & Carbonell, E. (2010). Middle Pleistocene lower back and pelvis from an aged human individual from the Sima de los Huesos site, Spain. *Proceedings of the National Academy of Sciences of the United States of America*, *107*, 18386–18391.

Bookstein, F. L. (1991). *Morphometric tools for landmark data geometry and biology*. Cambridge University Press.

Boule, M. (1911). *L'Homme Fossile de La Chapelle aux Saints*. Annales de Paléontologie, Masson et C Editeurs.

Buck, L. T., & Stringer, C. B. (2014). *Homo heidelbergensis*. *Current Biology*, *24*(6), 214–215.

Cabo, L. L., Brewster, C. P., & Luebo-Azpiazu, J. (2015). Sexual dimorphism interpreting sex markers. In D. C. Dirkmaat (Ed.), *A companion to forensic anthropology* (pp. 248–286). Wiley Blackwell.

Carretero, J. M. (1994). *Estudio del esqueleto de las dos cinturas y el miembro superior de los homínidos de la Sima de los Huesos sierra de Atapuerca Burgos (study of the skeleton of the two girdles and the upper limb of the hominids from the Sima de los Huesos Sierra de Atapuerca Burgos)*. PhD University Complutense of Madrid.

Carretero, J. M., Arsuaga, J. L., Martinez, I., Quam, R. M., Lorenzo, C., Gracia-Téllez, A., & Ortega, A. I. (2004). Los humanos de la Sima de los Huesos (Sierra de Atapuerca) y la evolución del cuerpo del género *Homo*. In E. Baquedano & S. Rubio (Eds.), *Miscelanea en Homenaje a Emiliano Aguirre, Zona Arqueologica* (pp. 120–135). Alcalá de Henares.

Carretero, J. M., Lorenzo, C., & Arsuaga, J. L. (1999). Axial and appendicular skeleton of *Homo antecessor*. *Journal of Human Evolution*, *37*(3–4), 459–499.

Carretero, J. M., Rodríguez, L., García-González, R., & Arsuaga, J. L. (2015). Estimated body parameters of the Sima de los Huesos hominins. *American Journal of Physical Anthropology*, *156*, 102.

Carretero, J. M., Rodríguez, L., García-González, R., Arsuaga, J. L., Gómez-Olivencia, A., Lorenzo, C., Bonmatí, A., Gracia, A., Martínez, I., & Quam, R. (2012). Stature estimation from complete long bones in the Middle Pleistocene humans from the Sima de los Huesos Sierra de Atapuerca (Spain). *Journal of Human Evolution*, *62*, 242–256.

Carretero, J. M., Rodríguez, L., Quam, R. M., García-González, R., & Arsuaga, J. L. (2018). Exploring bone volume and skeletal weight in the Middle Pleistocene Humans from Sima de los Huesos site (Sierra de Atapuerca Spain). *Journal of Anatomy*, *233*, 740–754.

Cavaignac, E., Savall, F., Faruch, M., Reina, N., Chiron, P., & Telmon, N. (2016). Geometric morphometric analysis reveals sexual dimorphism in the distal femur. *Forensic Science International*, *259*, 2461–2465.

Chevalier, T., & de Lumley, M.-A. (2018). Les fémurs Laz 13, Laz 15 et Laz 17, Laz 25 de la grotte du Lazaret. In M.-A. Lumley (Ed.), *Les restes humains fossiles de la grotte du Lazaret, Nice, Alpes-Maritimes, France, Des Homo erectus européens évolués en voie de néandertalisation, Chapitre XV* (pp. 435–468). CNRS Éditions.

Chevalier, T., & de Lumley, M. A. (2022). Lower limb bone structure of Middle Pleistocene hominins from the Caune de l'Arago (Tautavel, France): Evolutionary and functional comparison with the penecontemporaneous hominins of Sima de los Huesos (Atapuerca, Spain). *L'Anthropologie*, *126*(4), 103065.

Churchill, S. E. (1998). Cold adaptation heterochrony and Neandertals. *Evolutionary Anthropology*, *7*, 46–60.

Cross, M. J., & Waldrop, J. (1975). Thepatella index as a guide to the understanding and diagnosis of patellofemoralinstability. *Clinical Orthopaedics and Related Research*, *110*, 174–176.

Currey, J. D. (2002). *Bones: Structure and mechanics*. Princeton University Press Princenton.

Day, M. (1971). Postcranial remains of *Homo erectus* from bed IV Olduvai Gorge Tanzania. *Nature*, *232*, 383–387.

De Groote, I. (2011). Femoral curvature in Neanderthals and modern humans: A 3D geometric morphometric analysis. *Journal of Human Evolution*, *60*, 540–548.

Dejour, H., Walch, G., Nove-Josserand, L., & Guier, C. H. (1994). Factors of patellar instability: An anatomic radiographicstudy. *Knee Surgery, Sports Traumatology, Arthroscopy*, *2*, 19–26.

Dittrick, J., & Suchey, J. M. (1986). Sex determination of prehistoric Central California skeletal remains using discriminant analysis of the femur and humerus. *American Journal of Physical Anthropology*, *70*, 3–9.

Endo, B., & Kimura, T. (1970). Postcranial skeleton of the Amud man. In H. Suzuki & F. Takai (Eds.), *The Amud man and his cave site* (pp. 231–406). Academic Press of Japan.

Feldesman, M. R. (1992). Femur/stature ratio and estimates of stature in children. *American Journal of Physical Anthropology*, *87*, 447–459.

Fucentese, S. F., von Roll, A., Koch, P. P., Epari, D. R., Fuchs, B., & Schottle, P. B. (2006). The patella morphology in trochlear dysplasia—a comparative MRI study. *Knee*, *13*(2), 145–150.

Formicola, V. (2003). More is not always better: Trotter and Gleser's equations and stature estimates of upper Paleolithic European samples. *Journal of Human Evolution*, *45*, 239–244.

Friedl, L., Eisová, S., & Holliday, T. W. (2016). Re-evaluation of Pleistocene and Holocene long bone robusticity trends with regards to age-at-death estimates and size standardization procedures. *Journal of Human Evolution*, *97*, 109–122.

García-Campos, C., Modesto-Mata, M., Martinón-Torres, M., Martínez de Pinillos, M., Martín-Francés, L., Arsuaga, J. L., &

Bermúdez de Castro, J. M. (2020). Sexual dimorphism of the enamel and dentine dimensions of the permanent canines of the Middle Pleistocene hominins from Sima de los Huesos (Burgos Spain). *Journal of Human Evolution*, *144*, 102793.

García-González, R. (2013). *Estudio comparativo de los patrones de crecimiento y desarrollo corporal en humanos actuales y fósiles a partir del análisis de los huesos largos (comparative study of body growth and development patterns based on the analysis of long bones in present-day and fossil humans)*. PhD University of Burgos.

García-González, R., Rodríguez, L., Salazar-Fernández, A., Arsuaga, J. L., & Carretero, J.-M. (2024). Updated study of adult and subadult pectoral girdle bones from Sima de los Huesos site (Sierra de Atapuerca, Burgos, Spain). Anatomical and age estimation keys. *The Anatomical Record*, *307*(7), 2491–2518. https://doi.org/10.1002/ar.25158

García-Martínez, D., Barash, A., Recheis, W., Utrilla, C., Torres-Sánchez, I., García-Río, F., & Bastir, M. (2014). On the chest size of Kebara 2. *Journal of Human Evolution*, *70*, 69–72.

Ghosh, S., Sethi, M., & Vasudeva, N. (2014). Incidence of third trochanter and hypotrochanteric fossa in human femora in Indian population. *OA Journal of Case Reports*, *3*, 2–14.

Gilbert, W. H. (2008). Daka member hominid postcranial remains. In W. H. Gilbert & B. Asfaw (Eds.), *Homo erectus Pleistocene evidence from the Middle Awash*. Ethiopia University of California Press.

Gómez-Olivencia, A., Barash, A., García-Martínez, D., Arlegi, M., Kramer, P., Bastir, M., & Been, E. (2018). 3D virtual reconstruction of the Kebara 2 Neandertal thorax. *Nature Communications*, *9*, 4387.

Gómez-Olivencia, A., Eaves-Johnson, K. L., Franciscus, R. G., Carretero, J. M., & Arsuaga, J. L. (2009). Kebara 2: New insights regarding the most complete Neandertal thorax. *Journal of Human Evolution*, *57*, 75–90.

Grine, F. E., Jungers, W. L., Tobias, P. V., & Pearson, O. M. (1995). Fossil *Homo* femur from Berg Aukas Northern Namibia. *American Journal of Physical Antrhopology*, *97*, 151–185.

Heim, J. L. (1982). *Les Hommes fossiles de la Ferrasie Archives de l'Institut de Paléontologie Humaine*. Masson.

Hills, M. (1978). On ratios—A response to Atchley Gaskins and Anderson. *Systematic Zoology*, *27*(1), 61–62.

Holliday, T. W. (1997). Postcranial evidence and cold adaptation in European Neandertals. *American Journal of Physical Anthropology*, *104*, 245–258.

Holliday, T. W. (2012). Body size body shape and the circumscription of the genus *Homo*. *Current Anthropology*, *53*(S6), S330–S345.

Holliday, T. W., & Ruff, C. B. (2001). Relative variation in human proximal and distal limb segment lengths. *American Journal of Physical Anthropology*, *116*, 26–33.

Holt, B., & Whittey, E. (2019). The impact of terrain on lower limb bone structure. *American Journal of Physical Anthropology*, *168*(4), 729–743.

Holt, B. M. (2003). Mobility in upper Paleolithic and Mesolithic Europe: Evidence from the lower limb. *American Journal of Physical Anthropology*, *122*, 200–215.

Hrdlička, A. (1937). Gluteal ridge and gluteal tuberosities. *American Journal of Physical Anthropology*, *23*, 127–198.

Hrdlička, A. (1934). The hypotrochanteric fossa of the femur. *Smithsonian Miscellaneous Collections*, *92*(1), 1–63.

Institute for Analysis and Visualization. (2007). Landmark editor v.3.6. University of California, Davis.

İşcan, M. Y., & Shihai, D. (1995). Sexual dimorphism in the Chinese femur. *Forensic Science International*, *74*, 79–87.

Jantz, R. J., & Moore-Jansen, P. H. (2000). In T. Uo (Ed.), *Database for forensic anthropology in the United States 1962–1991 computer file*. Inter-university Consortium for Political and Social Research Knoxville.

Kapandji, A. I. (1996). *Cuadernos de fisiología articular: Miembro Inferior Cuadernos de fisiología articular*. Masson.

Kennedy, G. E. (1983). Some aspects of femoral morphology in *Homo erectus*. *Journal of Human Evolution*, *12*, 587–616.

Keppel, G. (1991). *Design and analysis: A researcher's handbook* (3rd ed.). Prentice-Hall, Inc.

Kim, D. I., Kwak, D. S., & Han, S. H. (2013). Sex determination using discriminant analysis of the medial and lateral condyles of the femur in Koreans. *Forensic Science International*, *233*, 121–125.

King, C., İşcan, M., & Loth, S. (1998). Metric and comparative analysis of sexual dimorphism in the Thai femur. *Journal of Forensic Science*, *43*, 954–958.

Klingenberg, C. P. (2011). MorphoJ: An integrated software package for geometric morphometrics. *Molecular Ecology Resources*, *11*, 353–357.

Klingenberg, C. P. (2015). Analyzing fluctuating asymmetry with geometric morphometrics: Concepts, methods, and applications. *Symmetry*, *7*, 843–934.

Klingenberg, C. P., Barluenga, M., & Meyer, A. (2002). Shape analysis of symmetric structures: Quantifying variation among individuals and asymmetry. *Evolution*, *56*, 1909–1920.

Klingenberg, C. P., & McIntyre, G. S. (1998). Geometric morphometrics of developmental instability: Analyzing patterns of fluctuating asymmetry with procrustes methods. *Evolution*, *52*, 1363–1375.

Kranioti, E. F., Vorniotakis, N., Galiatsou, C., İşcan, M. Y., & Michalodimitrakis, M. (2009). Sex identification and software development using digital femoral head radiographs. *Forensic Science International*, *189*, 1131–1137.

Kubicka, A. M., Balzeau, A., Kosicki, J., Nowaczewska, W., Haduch, E., Spinek, A., & Piontek, J. (2022). Variation in cross-sectional indicator of femoral robusticity in *Homo sapiens* and Neandertals. *Science Reports*, *12*(1), 1–13.

Lanyon, L. E. (1980). The influence of function on the development of bone curvature-an experimental study on the rat tibia. *Journal of Zoology*, *192*(DEC), 457–466.

Larsen, C. S., Ruff, C. B., & Kelly, R. L. (1995). Structural analysis of the Stillwater postcranial human remains: Behavioral implications of articular joint pathology and long bone diaphyseal morphology. In C. S. Larsen & R. L. Kelly (Eds.), *Bioarchaeology of stillwater marsch* (Vol. 77, pp. 107–133). Anthropological Papers of the AMNH.

Lesnik, J. J., & Sams, A. J. (2014). Using resampling statistics to test male interment bias: Applications for looted and commingled prehistoric remains in Peru and the reassessment of Neandertal burials. *Palaeoantropology*, *2014*, 463–469.

Lorenzo, C., Carretero, J. M., Arsuaga, J. L., Gracia, A., & Martínez, I. (1998). Intrapopulational body size variation and cranial capacity variation in Middle Pleistocene humans: The Sima de los Huesos sample (Sierra de Atapuerca Spain). *American Journal of Physical Anthropology*, *106*, 19–33.

Lovejoy, C. O. (1975). *Biomechanical perspectives on the lower limb of early hominids. Primate functional morphology and evolution* (pp. 291–326). De Gruyter Mouton.

Lovejoy, C. O., Heiple, K. G., & Burstein, A. H. (1973). The gait of Australopithecus. *American Journal of Physical Anthropology*, *38*(3), 757–780.

Lovejoy, C. O., Johanson, D. C., & Coppens, Y. (1982). Hominid lower limb bones recovered from the Hadar Formation: 1974–1977 collections. *American Journal of Physical Anthropology*, *57*(4), 679–700.

Lovejoy, C. O., Meindl, R. S., Ohman, J. C., Heiple, K. G., & White, T. D. (2002). The Maka femur and its bearing on the antiquity of human walking: Applying contemporary concepts of morphogenesis to the human fossil record. *American Journal of Physical Anthropology*, *119*(2), 97–133.

de Lumley, M. A. (1972). L'os iliaque anténéandertalien de la Grotte du Prince (Grimaldi Ligurie italienne). *Bulletin du Musée d'Anthropologie Préhistorique de Monaco*, *18*, 89–112.

Mahfouz, M. R., Merkl, B. C., Abdel-Fatah, E. E., Booth, R., & Argenson, J. N. (2007). Automatic methods for characterization of sexual dimorphism of adult femora: Distal femur. *Computer Methods in Biomechanics and Biomedical Engineering*, *10*, 447–456.

Manzi, G. (2011). Before the emergence of *Homo sapiens*: Overview on the early-to-Middle Pleistocene fossil record (with a proposal about *Homo heidelbergensis* at the subspecific level). *International Journal of Evolutionary Biology*, *2011*, 1–11.

Marchi, D., Walker, C. S., Wei, P., Holliday, T. W., Churchill, S. E., Berger, L. R., & DeSilva, J. M. (2017). The thigh and leg of *homo Naledi*. *Journal of Human Evolution*, *104*, 174–204.

Mariotti, V., & Belcastro, M. G. (2011). Lower limb entheseal morphology in the Neandertal Krapina population (Croatia 130,000 BP). *Journal of Human Evolution*, *60*(6), 694–702.

Martin, R., & Saller, K. (1957). *Lehrbuch der Anthropologie*. Gustav Fischer Verlag.

McCown, T. D., & Keith, A. (1939). *The stone age of Mount Carmel II: The fossil human remains from the Levalloiso-Mousterian*. Clarendon Press.

Mitteroecker, P., & Gunz, P. (2009). Advances in geometric morphometrics. *Evolutionary Biology*, *36*, 235–247.

Mounier, A., Marchal, F., & Condemi, S. (2009). Is *Homo heidelbergensis* a distinct species? New insight on the Mauer mandible. *Journal of Human Evolution*, *56*(3), 219–246.

Niinimäki, S., Narra, N., Härk, L., & Abe, S. (2017). The relationship between loading history and proximal femoral diaphysis cross-sectional geometry. *American Journal of Human Biology*, *29*, 22965.

Olivier, G. (1960). *Practique antrhropologique*. Vigot.

O'Higgins, P. (2000). The study of morphological variation in the hominidfossil record: Biology, landmarks and geometry. *Journal of Anatomy*, *197*, 103–120.

Pearson, O. M. (2000). Activity climate and postcranial robusticity. *Current Anthropology*, *41*, 569–607.

Pearson, O. M., & Busby, A. M. (2006). Physique and ecogeographic adaptations of the last interglacial Neandertals from Krapina. *Periodicum Biologorum*, *108*, 449–455.

Pearson, O. M., & Lieberman, D. E. (2004). The aging of Wolff's"-law": Ontogeny and responses to mechanical loading in cortical bone. *American Journal of Physical Anthropology*, *125*(S39), 63–99.

Plavcan, J. M. (1994). Comparison of four methods for estimating sexual dimorphism in fossils. *American Journal of Physical Anthropology*, *94*, 465–476.

Plavcan, J. M. (2012). Body size size variation and sexual size dimorphism in early *Homo*. *Current Anthropology*, *53*, S409–S423.

Plavcan, J. M., Meyer, V., Hammond, A. S., Couture, C., Madelaine, S., Holliday, T. W., Maureille, B., Ward, C. V., & Trinkaus, E. (2014). The Regourdou 1 Neandertal body size. *Comptes Rendus Palevol*, *13*(8), 747–754.

Purkait, R. (2003). Sex determination from femoral head measurements: A new approach. *Legal Medicine*, *5*, S347–S350.

Purkait, R., & Chandra, H. (2004). A study of sexual variation in Indian femur. *Forensic Science International*, *146*, 25–33.

Qiu, L., Li, J., Sheng, B., Yang, H., Xiao, Z., Lv, F., & Lv, F. (2022). Patellar shape is associated with femoral trochlear morphology inindividuals with mature skeletal development. *BMC Musculoskeletal Disorders*, *23*(1), 56.

Rak, Y. (1990). On the differences between two pelvises of Mousterian context from the Qafzeh and Kebara caves Israel. *American Journal of Physical Anthropology*, *81*, 323–332.

Rak, Y. (1991). *The pelvis in: Le Squelette Moustérien de Kébara 2* (pp. 147–156). Centre National de la Recherche Scientifique.

Rak, Y., & Arensburg, B. (1987). Kebara 2 Neanderthal pelvis: First look at a complete inlet. *American Journal of Physical Anthropology*, *73*, 227–231.

Rodríguez, L. (2013). *Estudio biomecánico de los huesos largos del esqueleto apendicular de los homínidos del Pleistoceno Medio de la Sima de los Huesos Sierra de Atapuerca (Burgos): implicaciones paleobiológicas y filogenéticas (Biomechanical study of the long bones from the appendicular skeleton of the of Middle Pleistocene hominids from the Sima de los Huesos Sierra de Atapuerca (Burgos): Paleobiological and phylogenetic implications)*. PhD University of Burgos.

Rodríguez, L., Carretero, J. M., García-González, R., & Arsuaga, J. L. (2018). Cross-sectional properties of the lower limb long bones in the Middle Pleistocene Sima de los Huesos sample (sierra de Atapuerca Spain). *Journal of Human Evolution*, *117*, 1–12.

Rosas, A., Agustina, B. L., García-Martínez, D., Torres-Tamayo, N., García-Tabernero, A., Pastor, J. F., de la Rasilla, M., & Bastir, M. (2020). Analyses of the neandertal patellae from El Sidrón (Asturias, Spain) with implications for the evolution of body form in Homo. *Journal of Human Evolution*, *141*, 102738.

Rosenberg, K. R., Zuné, L., & Ruff, C. B. (2006). Body size body proportions and encephalization in a Middle Pleistocene archaic human from northern China. *Proceedings of the National Academy of Sciences of the United States of America*, *103*, 3552–3556.

Ruff, C. B. (1987). Sexual dimorphism in human lower limb bone structure: Relationship to subsistence strategy and sexual division of labor. *Journal of Human Evolution*, *16*, 391–416.

Ruff, C. B. (1991). Climate and body shape in hominid evolution. *Journal of Human Evolution*, *21*(2), 81–105.

Ruff, C. B. (1994). Morphological adaptation to climate in modern and fossil hominids. *American Journal of Physical Anthropology*, *37*(S19), 65–107.

Ruff, C. B. (1995). Biomechanics of the hip and birth in early *Homo*. *American Journal of Physical Anthropology*, *98*, 527–574.

Ruff, C. B. (2000). Body size body shape and long bone strength in modern humans. *Journal of Human Evolution*, *38*(2), 269–290.

Ruff, C. B. (2005). Mechanical determinants of bone form: Insights from skeletal remains. *Journal of Musculoskeletal and Neuronal Interactions*, *5*, 202–212.

Ruff, C. B. (2010). Body size and body shape in early hominins—Implications of the Gona pelvis. *Journal of Human Evolution*, *58*, 166–178.

Ruff, C. B. (2018a). In C. B. Ruff (Ed.), *Skeletal variation and adaptation in Europeans: Upper Paleolithic to the twentieth century*. Wiley Blackwell.

Ruff, C. B. (2018b). Biomechanical analyses of archaeological human skeletons. In M. A. Katzenberg & A. L. Grauer (Eds.), *Biological anthropology of the human skeleton* (pp. 189–224). John Wiley and Sons.

Ruff, C. B., Burgess, M. L., Squyres, N., Junno, J. A., & Trinkaus, E. (2018). Lower limb articular scaling and body mass estimation in Pliocene and Pleistocene hominins. *Journal of Human Evolution*, *115*, 85–111.

Ruff, C. B., & Niskanen, M. (2018). Introduction to special issue: Body mass estimation–methodological issues and fossil applications. *Journal of Human Evolution*, *115*, 1–7.

Ruff, C. B., Niskanen, M., Junno, J., & Jamison, P. (2005). Body mass prediction from stature and bi-iliac breadth in two high latitude populations with application to earlier higher latitude humans. *Journal of Human Evolution*, *48*, 318–392.

Ruff, C. B., Puymerail, L., Macchiarelli, R., Sipla, J., & Ciochon, R. L. (2015). Structure and composition of the Trinilfemora: Functional and taxonomic implications. *Journal of Human Evolution*, *80*, 147–158.

Ruff, C. B., Scott, W. W., & Liu, A. Y. (1991). Articular and diaphyseal remodeling of the proximal femur with changes in body mass in adults. *American Journal of Physical Anthropology*, *86*, 397–413.

Ruff, C. B., Trinkaus, E., & Holliday, T. W. (1997). Body mass and encephalization in Pleistocene homo. *Nature*, *387*, 173–176.

Ruff, C. B., Trinkaus, E., Walker, A., & Larsen, C. S. (1993). Postcranial robusticity in homo I: Temporal trends and mechanical interpretation. *American Journal of Physical Anthropology*, *91*, 21–53.

Shackelford, L., & Trinkaus, E. (2002). Late Pleistocene human femoral diaphyseal curvature. *American Journal of Physical Anthropology*, *118*, 359–370.

Shaw, C. N., & Stock, J. T. (2010). The influence of body proportions on femoral and tibial midshaft shape in hunter-gatherers. *American Journal of Physical Anthropology*, *144*, 22–29.

Sládek, V., Berner, M., & Sailer, R. (2006). Mobility in central European late eneolithic and early bronze age: Femoral cross-sectional geometry. *American Journal of Physical Anthropology*, *130*, 320–332.

Slice, D. E. (2007). Geometric morphometrics. *Annual Review of Anthropology*, *36*, 261–281.

Smith, R. J. (2005). Relative size versus controlling for size: Interpretation of ratios in research on sexual dimorphism in the human corpus callosum. *Current Anthropology*, *46*, 249–273.

Srivastava, R., Saini, V., Rai, R. K., Pandey, S., & Tripathi, S. K. (2012). A study of sexual dimorphism in the femur among north Indians. *Journal of Forensic Science*, *57*, 19–23.

Steyn, M., & İşcan, M. Y. (1997). Sex determination from the femur and tibia in South African whites. *Forensic Science International*, *90*, 111–119.

Stock, J. T. (2006). Hunter-gatherer postcranial Robusticity relative to patterns of mobility climatic adaptation and selection for tissue economy. *American Journal of Physical Anthropology*, *131*, 194–204.

Stock, J. T., & Pfeiffer, S. K. (2004). Long bone robusticity and subsistence behaviour among later stone age foragers of the forest and fynbos biomes of South Africa. *Journal of Archaeological Science*, *31*, 999–1013.

Stringer, C. B. (2012). The status of *Homo heidelbergensis* (Schoetensack 1908). *Evolutionary Anthropology*, *21*, 101–107.

Swan, K. R., Ives, R., Wilson, L. A. B., & Humphrey, L. T. (2020). Ontogenetic changes in femoral cross-sectional geometry during childhood locomotor development. *American Journal of Physical Anthropology*, *173*, 80–95.

Tague, R. G. (1992). Sexual dimorphism in the human bony pelvis with a consideration of the Neandertal pelvis from Kebara cave Israel. *American Journal of Physical Anthropology*, *88*, 1–21.

Tamagnini, E., & Vierira de Campos, D. S. (1949). *Estudo da Antropologia Portuguesa IV: O femur Portugues*. Universidad de Coimbra.

Tattersall, I. (2011). *Before the Neanderthals: Hominid evolution in Middle Pleistocene Europe In continuity and discontinuity in the peopling of Europe* (pp. 47–53). Springer.

Trinkaus, E. (1975). The Neanderthals from Krapina northern Yugoslavia: An inventory of the lower limb remains. *Zeitschrift für Morphologie Und Anthropologie*, *67*, 44–59.

Trinkaus, E. (1976). The evolution of the hominid femoral diaphysis during the Upper Pleistocene in Europe and the Near East. *Zeitschrift für Morphologie Und Anthropologie*, *67*, 291–319.

Trinkaus, E. (1980). Sexual dimorphism in neanderthal limb bones. *Journal of Human Evolution*, *9*, 377–397.

Trinkaus, E. (1983). *The Shanidar Neandertals*. Academic Press.

Trinkaus, E. (1993). Femoral neck-shaft angles of the quafzeh-Skhul early modern humans and the activity levels among immature near eastern Middle paleolithic hominids. *Journal of Human Evolution*, *25*, 393–416.

Trinkaus, E. (2000). Human patellar articular proportions: Recent and Pleistocene patterns. *Journal of Anatomy*, *196*, 473–483.

Trinkaus, E. (2006). The lower limb remains. In *Early modern human evolution in Central Europe: The people of Dolní Vestonice and Pavlov*. Oxford University Press.

Trinkaus, E. (2016). *The Krapina human postcranial remains: Morphology morphometrics and paleopathology*. Faculty of Humanities and Social Sciences University of Zagreb eds.

Trinkaus, E., Churchill, S. E., Ruff, C. B., & Vandermeersch, B. (1999). Long bone shaft Robusticity and body proportions of the Saint-Césaire 1 Châtelperronian Neanderthal. *Journal of Archaeological Science*, *26*, 753–773.

Trinkaus, E., & Ruff, C. B. (1999). Diaphyseal cross-sectional geometry of near eastern Middle Paleolithic humans: The femur. *Journal of Archaeological Science*, *26*(4), 409–424.

Trinkaus, E., & Ruff, C. B. (2012). Femoral and tibial diaphyseal cross-sectional geometry in Pleistocene *Homo*. *Palaeoanthropology*, *2012*, 13–62.

Trinkaus, E., Ruff, C. B., & Churchill, S. E. (1998). Upper limb versus lower limb loading patterns among near Middle paleolithic hominids. In T. Akazawa, K. Aoki, & O. Bar-Yosef (Eds.),

Neandertals and modern humans in Western Asia (pp. 391–405). Plenum Press.

Trinkaus, E., Ruff, C. B., Churchill, S. E., & Vandermeersch, B. (1998). Locomotion and body proportions of the Saint-Césaire 1 Châtelperronian Neandertal. *Proceedings of the National Academy of Sciences of the United States of America*, *95*, 5836–5840.

Trinkaus, E., Ruff, C. B., & Conroy, G. C. (1999). The anomalous archaic *Homo* femur from Berg Aukas Namibia. A biomechanical assessment. *American Journal of Physical Anthropology*, *110*, 379–391.

Van Gerven, D. P. (1972). The contribution of size and shape variation to patterns of sexual dimorphism of the human femur. *American Journal of Physical Anthropology*, *37*, 49–60.

Walmsley, T. (1933). The vertical axes of the femur and their relations. A contribution to the study of the erect position. *Journal of Anatomy*, *67*(2), 284–300.

Weaver, T. D. (2003). The shape of the Neandertal femur is primarily the consequence of a hyperpolar body form. *Proceedings of the National Academy of Sciences of the United States of America*, *100*, 6926–6929.

Weaver, T. D. (2009). The meaning of Neandertal skeletal morphology. *Proceedings of the National Academy of Sciences of the United States of America*, *106*, 16028–16033.

Weidenreich, F. (1941). The extremity bones of *Sinanthropus pekinensis*. *Paleontologia Sinica*, *5*, 373–383.

Wolpoff, M. H. (1978). Some implications of relative Biornechanical neck length in hominid femora. *American Journal of Physical Anthropology*, *48*, 143–148.

Yoshikawa, T., Turner, C. H., Peacock, M., Slemenda, C. W., Weaver, C. M., Teegarden, D., MArkwardt, D. V., & Burr, D. B. (1994). Geometric structure of the femoral neck measured using dual-energy X-ray absorptiometry. *Journal of Bone and Mineral Research*, *9*(7), 1053–1064.

Zaffagnini, S., Grassi, A., Zocco, G., Rosa, M. A., Signorelli, C., & Muccioli, G. M. M. (2017). The patellofemoral joint: From dysplasia to dislocation. *EFORT Open Reviews*, *2*(5), 204–214.

Zelditch, M. L., Lundrigan, B. L., & Garland, T. (2004). Developmental regulation of skull morphology. I. Ontogenetic dynamics of variance. *Evolution and Development*, *6*, 194–206.

How to cite this article: Carretero, J.-M., Rodríguez, L., García-González, R., & Arsuaga, J.-L. (2024). Main morphological characteristics and sexual dimorphism of hominin adult femora from the Sima de los Huesos Middle Pleistocene site (Sierra de Atapuerca, Spain). *The Anatomical Record*, *307*(7), 2575–2605. https://doi.org/10.1002/ar.25331